Ecological Modelling 440 (2021) 109352

Contents lists available at ScienceDirect

Ecological Modelling

journal homepage: www.elsevier.com/locate/ecolmodel

Individual-based model of population dynamics in a sea urchin of the Kerguelen Plateau (Southern Ocean), *Abatus cordatus*, under changing environmental conditions

Margot Arnould-Pétré [a,*], Charlène Guillaumot [a,b], Bruno Danis [b], Jean-Pierre Féral [c], Thomas Saucède [a]

[a] UMR 6282 Biogéosciences, Univ. Bourgogne Franche-Comté, CNRS, EPHE, 6 bd Gabriel F-21000 Dijon, France
[b] Laboratoire de Biologie Marine, Université Libre de Bruxelles, Avenue F.D.Roosevelt, 50. CP 160/15. 1050 Bruxelles, Belgium
[c] Aix Marseille Université/CNRS/IRD/UAPV, IMBE-Institut Méditerranéen de Biologie et d'Ecologie marine et continentale, UMR 7263, Station Marine d'Endoume, Chemin de la Batterie des Lions, 13007 Marseille, France

ARTICLE INFO

Keywords:
Ecological modelling
Kerguelen
Climate change
Model sensitivity
Endemic echinoderm
Dynamic energy budget
Individual-based model

ABSTRACT

The Kerguelen Islands are part of the French Southern Territories, located at the limit of the Indian and Southern oceans. They are highly impacted by climate change, and coastal marine areas are particularly at risk. Assessing the responses of species and populations to environmental change is challenging in such areas for which ecological modelling can constitute a helpful approach. In the present work, a DEB-IBM model (Dynamic Energy Budget – Individual-Based Model) was generated to simulate and predict population dynamics in an endemic and common benthic species of shallow marine habitats of the Kerguelen Islands, the sea urchin *Abatus cordatus*. The model relies on a dynamic energy budget model (DEB) developed at the individual level. Upscaled to an individual-based population model (IBM), it then enables to model population dynamics through time as a result of individual physiological responses to environmental variations. The model was successfully built for a reference site to simulate the response of populations to variations in food resources and temperature. Then, it was implemented to model population dynamics at other sites and for the different IPCC climate change scenarios RCP 2.6 and 8.5. Under present-day conditions, models predict a more determinant effect of food resources on population densities, and on juvenile densities in particular, relative to temperature. In contrast, simulations predict a sharp decline in population densities under conditions of IPCC scenarios RCP 2.6 and RCP 8.5 with a determinant effect of water warming leading to the extinction of most vulnerable populations after a 30-year simulation time due to high mortality levels associated with peaks of high temperatures. Such a dynamic model is here applied for the first time to a Southern Ocean benthic and brooding species and offers interesting prospects for Antarctic and sub-Antarctic biodiversity research. It could constitute a useful tool to support conservation studies in these remote regions where access and bio-monitoring represent challenging issues.

1. Introduction

The Kerguelen Islands are part of the French Southern Territories (Terres australes françaises - Taf), located at the limit of the Indian and Southern oceans, in the sub-Antarctic area. The region is highly impacted by climate change, and coastal marine ecosystems and habitats are particularly at risk given that species have long adapted to cold and stable conditions (Convey and Peck 2019; Gutt et al., 2018; Waller et al., 2017). Coastal marine species of the Kerguelen Islands are threatened by temperature and seasonality shifts, which are expected to intensify in a near future (Turner et al., 2014, IPCC 5th report Pachauri and Meyer, 2014). Future predictions of the Intergovernmental Panel on Climate Change (IPCC 5th report Pachauri and Meyer, 2014) are provided as possible Representative Concentration Pathways (RCP) scenarios of climate change and can be used to infer the potential response of ecosystems to future environmental conditions. However, the insufficient spatial and time resolutions of such models constitute serious limitations to assessing the effects of future environmental changes on sub-Antarctic species (Constable et al., 2014; Murphy and Hofmann 2012).

* Corresponding author.
E-mail address: m.arnould-petre@nhm.ac.uk (M. Arnould-Pétré).

https://doi.org/10.1016/j.ecolmodel.2020.109352
Received 30 January 2020; Received in revised form 14 October 2020; Accepted 23 October 2020
Available online 22 November 2020

The echinoid *Abatus cordatus (Verrill 1876)* is endemic to the Kerguelen oceanic plateau and common in coastal benthic habitats of the Kerguelen Islands. It is reported in the northern Kerguelen plateau, and around Heard and Kerguelen islands but most records are from shallow, coastal areas of the Kerguelen Islands where dense populations are commonly observed (Agassiz, 1881; De Ridder et al., 1992; David et al., 2005; Guillaumot et al., 2016, 2018b, 2018a; Hibberd and Moore, 2009; Mespoulhé, 1992; Poulin, 1996). This makes the species particularly at risk considering the synergetic effects of the multiple factors (temperature variations, significant shifts in coastal currents, sedimentation rates and phytoplanktonic blooms) affecting coastal marine communities at high latitudes (Gutt et al., 2018; Stenni et al., 2017; Waller et al., 2017). The species' endemicity can be partly related to low dispersal capabilities, which is a consequence of a particular life trait: *A. cordatus* broods its young in incubating pouches located on the aboral side of the test, and has a direct development with no larval stage and no metamorphosis. The low dispersal capacity of *A. cordatus* likely increases its vulnerability to environmental changes (Ledoux et al., 2012).

Benthic fauna of sub-Antarctic regions remains under-studied compared to pelagic species (Améziane et al., 2011; Xavier et al., 2016). Ecological niche models can represent relevant tools to study the consequences of environmental changes on the biology of these benthic organisms and on their population dynamics. Correlative niche models were used to predict the distribution of suitable areas for *A. cordatus* on the Kerguelen plateau (Guillaumot et al., 2018a,b). However, supplementary data and analyses are still needed to depict and understand the species' response to environmental changes.

In the present work, a mechanistic modelling approach using a Dynamic Energy Budget - Individual-Based Model (DEB-IBM) was used to analyse the biological response of *A. cordatus* to various environmental conditions. An individual mechanistic model (DEB) was first built using experimental and literature data (Guillaumot, 2019). A DEB model aims to represent the physiological development of an organism, from the embryo to its death based on energetic fluxes and allows considering the metabolic state of the individual at any given moment of its life cycle. It relies on biological principles and first laws of thermodynamics to recreate the metabolic development as a function of two environmental parameters, food resources and temperature (Kooijman, 2010).

The DEB model was then upscaled to the population level (IBM), wherein it was implemented as iterative mathematical calculations of each organism's individual development in the population. The IBM relies on the simulation of individuals as autonomous entities forming a complex population within a dynamic system (Railsback and Grimm, 2019). The DEB-IBM is used to analyse population dynamics emerging from the development and the physiological traits of individuals as a function of environmental forcing variables (i.e. food resources and temperature). The DEB-IBM can then be used to simulate population dynamics under different environmental scenarios, enabling a better quantification of the vulnerability of populations to changing environmental conditions.

Modelling population dynamics using a DEB-IBM model for a sub-Antarctic and brooding invertebrate brings a feature so far unseen in other published DEB models. The main objectives of the study were to develop a DEB-IBM model for *A. cordatus* (1) to simulate population structure and dynamics at different sites under both current environmental conditions and future IPCC climate scenarios RCP 2.6 and RCP 8.5, and (2) to assess the feasibility of such a model for organisms in a region where low data availability and resolution may limit model building and validation. The current resolution and accuracy of future climate scenarios in sub-Antarctic areas do not allow building precise and reliable predictions for the future but they were used here as a proof of concept to test population responses to various, conceivable conditions. Sensitivity analyses were performed to test the robustness, potential and relevance of models (Grimm and Berger 2016) considering data availability. Simulations performed for various temperature conditions and food resource availabilities, if validated, may constitute a promising tool to address conservation issues.

2. Methods

2.1. Study area

The DEB-IBM population model was generated in the geographic and environmental context of the Kerguelen Islands (Fig. 1) using data of the study site of Anse du Halage, a fieldwork station that has regularly been investigated through several biological studies since the 1980s (Magniez, 1980; Mespoulhé, 1992; Schatt and Féral 1991, Poulin 1995, Ledoux et al., 2012, Poulin and Féral 1998). The Kerguelen Islands show jagged coastlines and numerous islets and fjords that provide a large variety of habitats to the marine benthic fauna. The nature of the seafloor varies from rocky to sandy and muddy shores. The predominance of the giant kelp *Macrocystis pyrifera* is a main feature of the Kerguelen as this engineer and key species plays a decisive role in the protection and structuring of benthic shallow habitats in many places of the archipelago (Arnaud, 1974; Féral et al., 2019; Lang, 1967, 1971).

Located in the Morbihan Bay, a 700 km^2 semi-enclosed shallow embayment (50 m depth on average) of the Kerguelen Islands, Anse du Halage is situated at the bottom of a small and shallow (2 m depth) cove dominated by fine to medium sands (Magniez, 1979; Poulin, 1996) (Fig. 1). The tidal range is comprised between 0.4 and 2.1 m, so that the area can exceptionally be uncovered at the lowest tides (Mespoulhé, 1992; Schatt and Féral, 1991). Sea surface temperature varies between 1 and 2 °C in winter (September) to 7 to 8 °C in summer (March), with sporadic peaks of +11 °C in some places for certain years (Féral et al., 2019; Schatt and Féral, 1991). Salinity varies between 31.89 and 33.57 (Arnaud, 1974).

Temperature data used in the model were collected in the framework of the Proteker programme (French Polar Institute n°1044) (Féral et al., 2019) and accessed online (IPEV programme n°1044, http://www.proteker.net/-Thermorecorders-.html?lang=en accessed on 08/05/2019). They were recorded from 2012 to 2018 at three sites used in the model

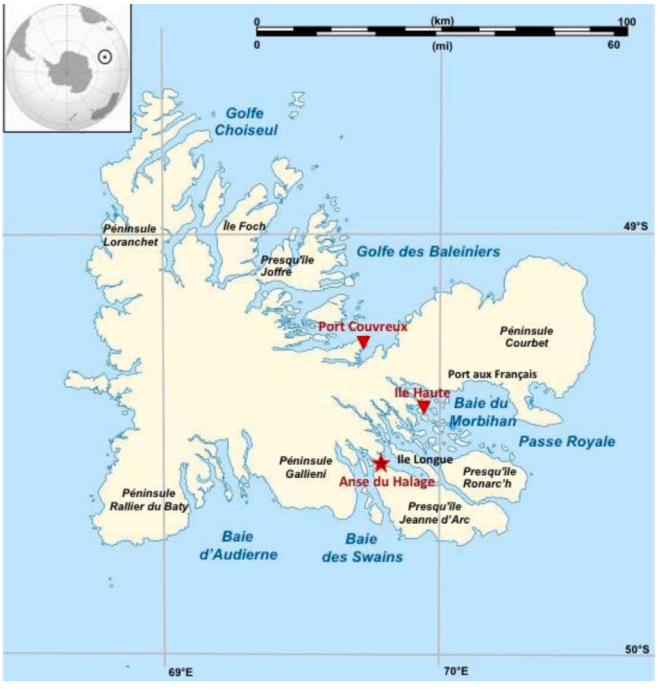

Fig. 1. Location of the studied sites in the Kerguelen Islands, calibration site (Anse du Halage, red star) and projection sites (Ile Haute and Port Couvreux, red triangles). (For interpretation of the references to colour in this figure legend, the reader is referred to the web version of this article.)

(Fig. 1): Ile Longue (for the model at Anse du Halage), Ile Haute, an island in the North-Western corner of the Morbihan Bay, and Port Couvreux, a coastal site outside the Morbihan Bay, in the Gulf of the Baleiniers on the Northern coast of the archipelago (Fig. A.1; see supplementary materials for all figures indexed by a letter).

The organic matter deposited on the seabed varies with seasonal phytoplankton blooms and remineralization by bacteriae (Delille et al., 1979). The sediment organic content and phytoplanktonic blooms are particularly important at Anse du Halage, with average values of 4.5% of organic carbon content. The sediment organic carbon (OC) content was measured monthly as a percentage of sediment dry weight by Delille and Bouvy (1989).

Environmental data time-series are available at a monthly timestep. The model was scaled on a single square metre patch, supposing no connectivity between neighbour locations, as no data on horizontal nor vertical water movements and matter fluxes were available.

2.2. Study species

Abatus cordatus (Fig. 2) is a shallow deposit-feeder and sediment swallower, living at 5 °C average, full or half buried into soft sediments (De Ridder and Lawrence, 1982). It is distributed all around the Kerguelen Islands, but population densities are highly variable depending on depth, substrate nature and exposure to the open sea. Distributed from the intertidal area to the deep shelf over 500 m depth, populations highest densities are found in very shallow (0–2 m depth) and sheltered areas with soft bottoms of fine to medium sand (Poulin, 1996). In shallow areas, observed density vary from less than 5 individuals/m^2 (in the Fjord des Portes Noires, Poulin and Féral 1995) to 10 ind./m^2 (at Port-aux-Français, Mespoulhé, 1992), 130 ind./m^2 (Ile Haute, Mespoulhé, 1992, Poulin, 1996), 168 ind./m^2 (Port Couvreux, Poulin, 1996) and up to 280 ind./m^2 (Anse du Halage, Magniez, 1980, Poulin, 1996). Juveniles are commonly found sheltered in between holdfasts of the giant kelp *Macrocystis pyrifera* bordering with sandy shallow areas.

The species is relatively resistant to low salinities locally induced by freshwater run-off from the main island (Guille and Lasserre 1979). It is tolerant to temperature variations, particularly marked in shallow areas, but temperature tolerance does not exceed +12 °C (personal observations). The maximum size ever observed is 4.9 cm in length (Mespoulhé, 1992). Lifespan is assumed to be around six years old (Mespoulhé, 1992), although it cannot be excluded that some individuals may grow older. Identified predators are gastropods, crustaceans and seagulls (Poulin, 1996; Poulin and Féral 1995) from which the specimens are hidden when burrowing into the sediment (Magniez, 1979; Poulin and Féral 1995).

Sexual reproduction in *A. cordatus* occurs every year, with all mature females producing eggs (Magniez, 1983) and incubating their young in their four brood pouches located on the aboral side of the test (Fig. 2b). After brooding, juveniles exit the pouches and start their autonomous development on the seabed, in the vicinity of their mother (Magniez, 1983; Schatt, 1985). Reproduction time can greatly differ between sites: generally extending from March to May (as in Anse du Halage and Ile Haute), reproduction can also occur from June to August (Ile Suhm), from December to February (Port Matha) or from August to November (Port Couvreux) (Poulin, 1996). Females usually spawn once a year (Poulin, 1996). Brooding and burrowing behaviours imply a relative sedentary lifestyle and can explain a part of the species endemicity, with dense populations scattered all around the archipelago and only a few older individuals that may be found isolated from core populations (Mespoulhé, 1992; Poulin and Féral 1995).

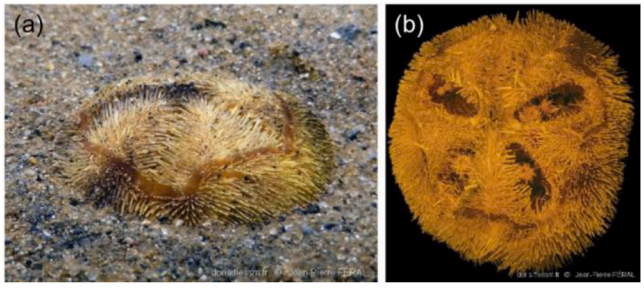

Fig. 2. Specimens of *Abatus cordatus*. (a) Aboral view of a specimen half buried in sand, (b) Aboral view of a female showing the brood pouches with juveniles inside. © Féral J.P.

2.3. DEB modelling

2.3.1. Principles

DEB theory defines individuals as dynamic systems and provides a mathematical framework for modelling organisms' life cycle. It describes physiological processes using four primary state variables —reserve, structure, reproduction buffer and maturity— directly linked to mass and energy flows and influenced by two forcing variables, temperature and food availability (Fig. 3, Jusup et al., 2017; Kooijman, 2010). Based on feeding, growth and reproduction processes, DEB models predict the metabolic and development states of organisms through time (Kooijman, 2010; Sousa et al., 2008). Metabolic processes are linked to shape and size of the organism, represented by the structural volume and the structural area. Structural volume is related to maintenance processes, while structural area is closely linked to food ingestion and assimilation processes and controls the amount of energy arriving into the reserve compartment *E* (Fig. 3A, van der Meer, 2006).

The energy contained in the reserve compartment is allocated to

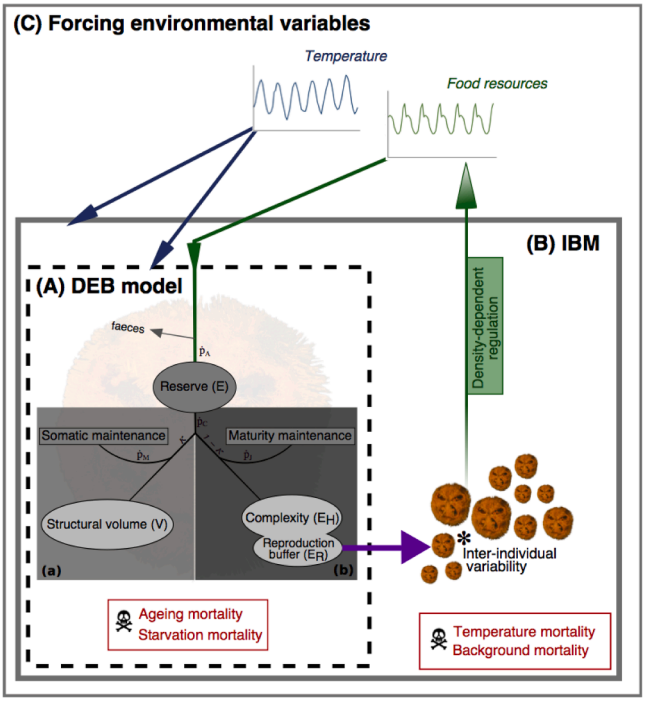

Fig. 3. Schematic representation of the DEB-IBM (Dynamic Energy Budget - Individual-Based Model). Individuals (A) undergo development through the DEB model and reproduce (purple arrow). Altogether and with a slight inter-individual variability in DEB parameters (*), they form the population of the IBM (B) which undergoes population-specific processes (temperature and background mortalities) at the scale of a simple square metre patch at the reference site (C). The IBM population is embedded within this specific environment, whose environmental conditions (temperature and food resources) affect individual and population dynamics. Additionally, the population influences the resources availability following a density-dependence regulation. (For interpretation of the references to colour in this figure legend, the reader is referred to the web version of this article.)

organism maintenance ('somatic' and 'maturity' maintenances, priority processes that condition the organism's survival), to growth (increase of structural volume V), and to the increase of complexity (E_H) or reproduction buffer (E_R) (Fig. 3A) according to the kappa-rule (Kooijman, 2010). The complexity is represented as the maturity level. The amount of energy accumulated into this compartment triggers metabolic switches such as the transition (i.e. ability to feed, to reproduce) between life stages, defined in DEB theory (namely embryo, juvenile and adult life stages) (Kooijman, 2010).

2.3.2. Application of DEB model to A. cordatus

Parameter estimation. An individual mechanistic DEB model was developed for *A. cordatus* (Guillaumot, 2019). Estimated DEB parameters are reported in Table 1. The DEB model considers a larval growth accelerated compared to the adult stage (Schatt, 1985), so-called 'abj' type model. The model was constructed using data from the literature (Table 2). The goodness of fit of the DEB model to the data was evaluated by calculating the Mean Relative Error (MRE) of each dataset, which is the sum of the absolute differences between observed and expected values, divided by the expected values. MRE values are contained in the interval [0, infinity). The MRE is considered to be a reference method to assess DEB modelling performance (Lika et al., 2011b), for which the closer to 0, the better model predictions match the data.

Maturation and development. Embryos of *A. cordatus* have a direct development in brood pouches of females (Magniez, 1983; Schatt, 1985). They start feeding inside pouches after 142 days of incubation (i.e. 5 months) and leave the pouches as fully developed sea urchins after 8.5 months (Schatt, 1985). According to DEB theory, individuals are considered embryos until they can feed (Kooijman, 2010). Before the fifth month, feeding inside the maternal pouches is not clearly attested, but feeding through epidermal uptake of Dissolved Organic Matter (DOM) is considered as the possible mechanism (Schatt and Féral 1996). At each growth step, energy is supplied to the reserve by the ingested food (Fig. 3A, $\dot{p}_A$) and then leaves the reserve compartment to be directed to growth, maturation or reproduction compartments through the mobilisation flux (Fig. 3A, $\dot{p}_C$). This is performed following the kappa-rule: a κ fraction is directed towards the structure (growth compartment and somatic maintenance, Fig. 3A(a)), and the remaining $1-\kappa$ fraction towards complexity (maturation, reproduction compartments and maturity maintenance, Fig. 3A(b)).

During the juvenile stage, the individual does not supply energy into reproduction, but accumulates energy in its maturity compartment E_H until reaching the 'puberty' threshold that, according to DEB theory, defines the moment when the organism is mature enough to reproduce (Kooijman, 2010). After reaching this threshold, at around 2.5 to 3 years old (Mespoulhé, 1992; Schatt, 1985), the organism can allocate energy into the reproduction buffer E_R for gamete production (Fig. 3A). The structural volume increases continuously along the individual's life, from birth to death, supplied in energy left from what has not been allocated to priority maintenance costs $\dot{p}_M$ and $\dot{p}_J$.

Starvation mortality. Magniez (1983) observed that the gonadal index continues to decrease slightly for around two months after reproduction. He hypothesized that it was related to the season: as the reproduction period finishes at the start of winter, food resources decrease and energy investment into reproductive organs is momentary diverted towards the maintenance of somatic elements. This was demonstrated in the other sea urchin species *Strongylocentrotus purpuratus* (Lawrence et al., 1966) and *Arbacia lixula* (Fenaux et al., 1975) confronted to starvation. In the model, when scaled reserve e (reserve relative to reserve capacity, no dimension) falls below the scaled structural length l (length relative to maximum length, no dimension), it is assumed that the individual is confronted to starvation: the kappa-rule is then altered as energy is entirely redirected to the somatic maintenance and all other fluxes (growth, reproduction or maturation) are set to 0. When $e < 0$, the organism does not have enough energy to allocate the amount necessary for survival (somatic maintenance costs) and dies. See section "7.Submodels/Starvation" in Appendix G for further details and implemented equations.

Ageing mortality. Death probability by senescence was calculated in the model using the ageing sub-model, a simulation of damages induced by lethal compounds such as free radical or other reactive oxygen species (ROS), following the DEB theory for ageing (Kooijman, 2010).

The density of damage inducing compounds in the body increases as the reserve compartment is fuelled with energy that is allocated through the entire organism. It influences the hazard mortality rate $\dot{h}$, which is a function of the damage accumulated in the body and simulates the vulnerability of the individual to damages, such as the risk of dying from illness increases with age. In the model, the hazard mortality rate $\dot{h}$ is supplemented by a stochastic parameter (Martin et al., 2010) to control the ageing mortality rate. See section "7.Submodels/Ageing" in Appendix G for further details and implemented equations.

Table 1
Parameters estimated for the DEB model developed for *Abatus cordatus*. Values are given for the reference temperature of 20 °C. The MRE of the model is 0.121.

Parameter	Symbol	Value	Unit
Basic DEB parameters			
Volume of specific somatic maintenance[1]	[pM]	13.84	$J.d^{-1}.$
Somatic maintenance rate coefficient[1]	kM	5.10^{-3}	cm^{-3}
Fraction of energy allocated to somatic maintenance and growth[1]	κ	0.78	d^{-1}
Volume-specific cost of structure[1]	$[E_H^b]$	2395	-
Energy of maturity at birth[1]	$[E_H^j]$	0.5693	$J.cm^{-3}$
Energy of maturity at metamorphosis[1]	$[E_H^p]$	8.325	$J.cm^{-3}$
Energy of maturity at puberty[1]	TA	1638	$J.cm^{-3}$
Arrhenius temperature[3]		9000	$J.cm^{-3}$
			K
DEB compound parameters			
Energy conductance[1]	$\dot{v}$	0.02722	$cm.d^{-1}$
Maturity maintenance rate coefficient[3]	kJ	0.002	d^{-1}
Shape coefficient[2]	δ	0.6718	-
Maximum structural length [1]	L_m	2.93	cm
Acceleration factor[1]	sM	2.397	-
Reproduction parameters			
Yield of structure on reserve[1]	yVE	0.865	#mol.
Contribution of reserve to weight[1]	w	0.647	mol^{-1}
			-
Ageing parameters			
Weibull ageing acceleration[1]	$\ddot{h}a$	$5.02.10^{-6}$	d^{-2}
Gompertz stress coefficient[3]	sG	0.0001	-

[1] Estimated using the covariation method (Lika et al., 2011a, 2011b; Marques et al., 2018).
[2] Calculated from data for initial value and then estimated with the covariation method.
[3] Fixed, guessed value.

2.4. Individual-based modelling for the population

2.4.1. Principles

The individual DEB model is used to simulate each individual as an entity of the individual-based population model (IBM). An IBM represents the individual components (individuals of *A. cordatus*) of an environmental system (Anse du Halage) and their behaviours, enabling to feature each individual as an autonomous entity and looking at results at the scale of the whole population (DeAngelis and Mooij 2005; Grimm and Railsback 2005; Railsback and Grimm 2019). In our model, each individual do not have any direct interaction nor adaptive behaviour towards their environment nor the other members of the population. They follow a continuous development governed by metabolic fluxes (DEB model) that are influenced by environmental conditions (temperature and food resources) along their entire life. Each individual is a component of the modelled population, which is itself affected by population death rate and density-dependant processes.

The IBM was built with the software Netlogo version 6.0.4 (Wilensky, 1999), using the DEB-IBM model developed by Martin et al. (2010)

Table 2
Zero and uni-variate data used for the estimation of the DEB model parameters. All values are given at a measured temperature of 5 °C. MRE: Mean Relative Error. Plots related to uni-variate data can be found in Appendix B.

Variable	Symbol	Obs.	Prediction	Unit	MRE	Reference
Zero-variate data						
Age at metamorphosis[1]	aj	142	143	d	0.0072	Schatt (1985)
Age at puberty[2]	ap	1098	1018	d	0.0731	Mespoulhé (1992)
Life span	am	2190	2190	d	5.10^{-8}	Mespoulhé (1992)
Length at metamorphosis	Lj	0.276	0.324	cm	0.1738	Schatt (1985)
Length at puberty	Lp	1.9	1.824	cm	0.0399	Mespoulhé (1992)
Maximal observed length (at 6 years old)	L6	4.2	3.65	cm	0.1321	Mespoulhé (1992)
Ultimate maximal length	Li	8	9.507	cm	0.1883	guessed
Wet weight of the egg	Ww0	$1.78.10^{-3}$	$1.59.10^{-3}$	g	0.1081	Schatt (1985)
Wet weight at metamorphosis	Wwj	$1.03.10^{-2}$	$1.70.10^{-2}$	g	0.6482	Schatt (1985)
Wet weight at puberty	Wwp	2.9	3.03	g	0.0448	Féral and Magniez (1988)
Wet weight at 6 years old	Ww6	25	24.18	g	0.0328	Féral and Magniez (1988)
Gonado-somatic index[3]	GSI	0.07	0.078	-	0.1194	Magniez (1983)
Variable	**Symbol**	**Obs. /Prediction**		**Unit**	**MRE**	**Reference**
Uni-variate data						
Time since birth vs. length	tL	See Appendix B	d // cm	0.2259	Schatt and Féral (1996)	
Egg diameter vs. egg wet weight	LW_egg		cm // g	0.1262	Mespoulhé (1992)	
Length vs. Wet weight adult	LW		cm // g	0.3248	Féral and Magniez (1988)	
Length vs. O2 consumption	LJO		cm // µL/h	0.2872	Féral and Magniez (1988)	

[1] moment at which the juveniles leave the brooding pouch of the mother.
[2] moment at which the sea urchin is able to reproduce.
[3] maximum gonad index for an animal of the maximum size, gonad index as gonad weight/total wet weight.

for the species *Daphnia magna*. The NetLogo code is available at http://modelingcommons.org/browse/one_model/6201. It contains the script to run the model, the input files of monthly food resources and temperatures for the three stations and a detailed description of the model following the ODD protocol from Grimm et al. (2010) and the associated list of variables present in the code. This detailed ODD was also included in Appendix G.

2.4.2. Application of IBM model to A. cordatus

Model structure. The model includes two types of entities: the individuals and the environment. Individuals are divided into 4 types of sub-agents, depending on their life stage and sex: embryos, juveniles, adult males and adult females. The values of four primary state variables are attributed to each individual (scaled reserve U_E, volumetric structural length L, scaled maturity U_H and scaled reproduction buffer U_R). The level of energy contained in the scaled maturity U_H thresholds the life stages. These four variables are 'scaled', meaning here that the energy dimension has been removed by dividing with the surface-area-specific maximum assimilation rate $\{\dot{p}_{Am}\}$ (in $J.L^{-2}.t^{-1}$), based on DEB theory (Kooijman, 2010).

Simulations were run with a monthly timestep for calculation, in regard to the slow growth of the species and the available data (an analysis of the effect of the timestep on the core individual model was conducted, cf. Appendix C). At each timestep, food and temperature conditions are first input into the model, state variable values of each individual are calculated in order to assess whether new maturity thresholds are reached or whether energy is sufficient for survival, growth or reproduction. The population state is reassessed at the end of each month. Spatially, population structure and density are simulated on a patch of one square metre at each site and individuals do not leave the patch during their entire life.

Initialisation. The initial population density value was set to 120 ind./m^2 and this figure was split into classes of equal densities of 20 individuals of different age-classes, between 0 and 5 years old, in order to stabilize the initialisation between the different replicates. An initial run is realised to capture the values of the four state variables that characterize the individual of each age class (at October 2012 temperatures and $f = 1$), in order to initiate the model (Appendix H).

The first decade of the simulation period was always considered as the initialisation phase and was removed from the analysis, the model showing important outliers (in individual metabolism and population structure) during these first ten years.

Inter-individuals variability. Each individual is characterized by similar energetic performances estimated by the DEB estimation (Table 1). Five DEB parameters were divided by a *scatter-multiplier* parameter that was generated in order to create inter-individual variability. These five DEB parameters were selected because they are associated to the four state variables that characterize the individuals and are not null at the time the individual is initiated into the model (following Martin et al., 2010): (1) maturity level at birth (U_H^b, $d.cm^2$), that is the amount of energy accumulated in the maturity compartment needed to reach the *juvenile*stage; (2) maturity level at *puberty* (U_H^p, $d.cm^2$), the amount of energy accumulated into the maturity compartment to reach the adult stage; (3) energy investment ratio (g,no dimension), the cost of the added volume relative to the maximum potentially available energy for growth and maintenance; (4) the initial energy reserve at *birth* (U_E, $d.cm^2$); and (5) the initial structural length (L, cm).

The *scatter-multiplier* is the exponential of a random number from a normal distribution of mean 0 and standard deviation *cv* (0.1 by default, can be set by the user in the interface of the model). The value is therefore small enough to not affect tremendously the initial variable and generate trade-off between parameters. It is applied as soon as the individual is created in the system.

Reproduction. Sex-ratios (ratio males/females) in the studied populations are slightly contrasting between localities, from 0.94 (Ile Haute) to 0.99 (Anse du Halage) and 1.04 (Port Couvreux) (Poulin, 1996). The average ratio of 0.99 was chosen in the model. By approximation, it was considered that only females undergo physiological changes during the reproduction process, males being only used as a component of the total population.

To this date, few monitoring studies have been performed on *A. cordatus* reproduction. Magniez (1983) is the only one who studied the Gonado Somatic Index (GSI), that is the proportion of ash-free gonads dry weight over the ash-free body dry weight, therefore directly linked to the accumulation of energy into the reproduction buffer. According to Magniez (1983), reproduction can occur if the GSI reaches at least 0.07%. This condition was used in our model to control the ability of the female to reproduce when time comes.

The gonadosomatic index GSI was only attributed to females and was estimated for each month, with this equation (Kooijman, 2010, section 4.10, eq. 4.89):

$$GSI = \frac{time\_of\_accumulation * \dot{k}_M * g}{f^3 * (f + \kappa * g * y_{VE})} * \left((1-\kappa) * f^3 - \frac{\dot{k}_J * U_H^p}{Lm^2 * s_M^3} \right),$$

where the time of accumulation is the number of days spent since the end of the reproduction period, $\dot{k}_M$ is the somatic maintenance rate coefficient (in d^{-1}), g the energy investment ratio (no dimension), f the scaled functional response (no dimension), κ the fraction of energy directed towards structure, y_{VE} the parameter for the yield of structure on reserve (mol/mol), that is the number of moles of structure that can be produced with one mole of reserve, $1 - \kappa$ the fraction of energy directed towards complexity, $\dot{k}_J$ the maturity maintenance rate coefficient (in d^{-1}), U_H^p the scaled energy in the complexity compartment at puberty ($d.cm^2$), L_m the maximum structural length (cm), and s_M the acceleration factor (no dimension).

The reproduction period is constant from March to May for the individuals at Anse du Halage, and they only spawn once a year (Magniez, 1983; Schatt and Féral 1996; Poulin, 1996). After each monthly step, the model checks the GSI value for each female. If the GSI reaches the 0.07% threshold at the onset of the period (March), reproduction is triggered for this considered female.

According to the literature, when reproducing, females invest around 52% of their reproductive organs' energy into reproduction (Magniez, 1983). This energy is released during the three months when spawning occurs. That is, the GSI of the female will decrease by 52% of its initial value over the 3 months period (so a decrease of one third of 52% per month, with $\partial GSI = (GSI_{start} - 0.52 * GSI_{start}) / 3$, where GSI_{start} is the level of gonadal index at the onset of reproduction). In parallel, the usual ∂U_R (change in energy density in the reproduction buffer outside of the reproduction period, no unit) is set to 0 for the three months, while U_R (energy density in the reproduction buffer) is forced to decrease in a similar fashion to the GSI: $\partial_2 U_R = (U_{R\_start} - 0.52 * U_{R\_start}) / 3$, with U_{R_start} being the reproduction buffer at the start of the period.

Reproduction induces the introduction of 27 embryos in average in the system (Magniez, 1983), added proportionally along the three months (9 per month).

Background mortality. No specific adult mortality rates are mentioned in the literature, as no cause have been defined precisely. Background population mortality annual rates were estimated based on size frequency distribution provided by Mespoulhé (1992), and using the formula from Ebert (2013) $N(t) = N_0 * e^{-M*t}$ with N(t) the population size at time t, N_0 the initial population size, M the mortality rate and t the time (in months). Two yearly mortality rates were defined: one for juveniles (41%) and one for adults (24%).

A percentage of embryos mortality in the pouches was calculated based on data from Poulin (1996), determining an egg survival of 65%. This mortality is associated to the fact that when the first juveniles start leaving the maternal pouches at the beginning of January, they push aside the protecting spikes of the pouch, and eggs remaining in the brood are no longer protected and die (Magniez, 1980).

Mortality induced by temperatures. As no precise information is available to accurately describe *A. cordatus* temperature tolerance, three different types of sensitivity were designed to cover different hypothesis (Fig. D.2). Based on experimental results obtained in the Kerguelen Islands (personal observation), mortality gradient due to temperature was applied to the population for temperatures comprised between 8 and 12 °C. Over 12 °C, all individuals are considered to die in the model, as none survived in the experiment. (1) A 'vulnerable' type was defined with population death rates of 25%, 35% and 45% when the sea urchins are exposed to temperatures respectively reaching 8, 9.5 and 11 °C during two consecutive months. (2) The 'resistant' type was defined with a mortality rate 15% lower than the vulnerable one for the same temperature thresholds (e.g. 10% instead of 25% population mortality at +8 °C), for similar exposure duration (i.e. two months). (3) The 'intermediate' type is similar to the 'resistant' type but individuals are considered to die after one month of exposure to each temperature instead of two (Fig. D.2).

Density-dependant regulation. Population density autoregulates through competition for food resources. This procedure relies on the monitoring of population density in relation to the carrying capacity and allows to stabilize the model. The model calculates the current population density and quantifies the competition effect on food availability depending on how far from the carrying capacity (K) the population density (P) is, and updates food availability in accordance.

It is considered that at each timestep, a certain amount of food is available in the environment (f_{env}) but according to population size, competition for food (FC, quantified food competition) is present and influences effective food availability (f_{eff}), with $f_{eff} = f_{env} + FC$, following Goedegebuure et al., 2018. f_{eff} and f_{env} are contained between 0 and 1. FC is calculated with the following equations:

$$\text{If } P < 1.9 * K, \text{ then } FC = (1 - f_{env}).\left(1 - \frac{P}{2.K - P}\right)$$

$$\text{If } P \geq 1.9 * K, \text{ then } FC = (1 - f_{env}).\left(1 - \frac{P}{K/10}\right)$$

FC is positive if $P < K$, and f_{eff} tends to its maximal value 1 with a decreasing population size, as FC becomes very low and tends to 1- f_{env}. When $P > K$, FC turns negative and makes f_{eff} decrease with the minimal value reached at $P = 2$ K.

Two equations are used because if $P = 2$ K, the first formula gives an error due to a division by 0, and if $P > 2$ K, then the formula gives the untrue result of less competition with a bigger population (hence the use of 1.9 as a pivot value). Competition is only effective if food availability is less than the maximum (hence the use of '1 - f_{env}' in the equation).

2.5. Summary of model parameterization and sensitivity analysis

The model was constructed following the ecological and physiological observations available in the literature for *A. cordatus*. These observations are summarised in the following table (Table 3). Once these elements added, the ageing submodel and the carrying capacity parameters, for which no in situ observations are defined, were calibrated until obtaining a model stable in time, over several centuries.

The sensitivity of the model to different parameters was tested. This sensitivity analysis also served as a first form of validation in the absence of wider means of validation. Initial population number, inter-individuals variation coefficient, juvenile and adult background mortalities, number of eggs produced per female during a reproduction event, and egg survival rate were each applied variations of −30%, −20%, −10%, +10%, +20% and +30% (Table 3). The influence of changes in these parameter values was assessed on the average population density (ind/m^2), the average juvenile/adult ratio, the average physical length, the average reserve energy and the average structural length variation over the period of 200 years. For each analysis, models were replicated 100 times. A model was considered to 'crash' when the population is not stable and collapses entirely before the end of the simulation period. The proportion of crashes relates to the number of crashes counted for 100 simulations (i.e., for 15 crashes and 100 simulations, the proportion is 15/(100+15)~13%). Due to computing time limitations, the analysis was stopped when reaching a proportion higher than 66% of crashes (indicated by a black cross in Appendix E).

The model sensitivity to the GSI threshold assumption was tested with the upper and lower values of the GSI calculated at the onset of reproduction in Magniez (1983). The minimum value did not impact the model at all, but the higher threshold value prevented most of the females from reproducing (results not presented).

2.6. Forcing environmental variables

2.6.1. Temperature

In the frame of DEB theory, temperature influences metabolic rates

Table 3
List of parameters integrated in the individual and population models. Descriptions and values. The source reference that justifies the choice of the parameterization is provided in the 'reference' column. The last column synthetises which parameters where modified to performed a sensitivity analysis, whose results are presented in Appendix E.

Parameters	Model parameterization	Reference	Sensitivity analysis
Individuals			
Time of development until birth	8 months	254 days (Schatt, 1985)	MRE DEB model
Time of development until puberty	Threshold by U_H^b value	2.5 to 3 years old (Schatt, 1985; Mespoulhé, 1992)	MRE DEB model
Starvation	$e < l$	Kooijman (2010)	Not tested
Ageing	Probability depending on accumulated cell damages, constrained by stochasticity	Damage probability: following Martin et al. (2010) and Kooijman (2010) rules for ageing Stochasticity: calibrated at the end of model construction until reaching model stability	Not tested, calibrated parameter
Population			
Initial population density	120 ind./m^2	Rounded from literature (Guille and Lasserre, 1979; Magniez, 1980; Mespoulhé, 1992; Poulin, 1996)	−30 to +30% variation tested
Initial population structure	5 age-classes of 20 individuals	Follow average population structure observed by Mespoulhé (1992)	Not tested
Variation coefficient (cv) from the inter-individual variability	0.1	Follow IBM parameterization of Martin et al. (2010) study	−30 to +30% variation tested
Ratio females/males	50/50	Sex-ratio: 0.99 (Poulin, 1996)	Not tested
Initial GSI	0.03%	Magniez (1983)	Not tested
GSI threshold for reproduction	0.07%	Magniez (1983)	Tested with the upper (0.116) and lower (0.028) values of the GSI calculated at the onset of reproduction in Magniez (1983)
Reproduction period	3 months once a year	Magniez (1983), Schatt and Féral (1996), Poulin (1996)	Not tested
Energy investment into reproduction	52% of the reproductive energy at the onset of the period	Magniez (1983)	Not tested
Number of eggs	27 eggs per adult female	Magniez (1983), Schatt (1985)	−30 to +30% variation tested
Eggs survival to juvenile stage (birth)	65%	Poulin (1996)	−30 to +30% variation tested
Yearly background mortality rates	41% of juveniles 24% of adults	Equation provided in Ebert et al. (2013), implemented with population data from Mespoulhé (1992)	−30 to +30% variation tested
Mortality induced by temperature tolerance	Three sensitivity scenarios	Designed from experimental results	Not tested
Carrying capacity	200 ind./m^2	Calibrated at the end of model construction until reaching model stability, no information available in the literature	Not tested, calibrated parameter

following the Arrhenius function which defines the range of temperatures that affect enzyme performance, considering that metabolic rates are controlled by enzymes that are set inactive beyond an optimal temperature tolerance (Kooijman, 2010; Thomas and Bacher 2018). The Arrhenius response is characterized by five parameters that describe the species tolerance range: the Arrhenius temperature T_A, the temperature at the upper and lower limits of the species tolerance range T_H and T_L respectively, and the Arrhenius temperature beyond upper and lower limits of the tolerance range T_{AH} and T_{AL} respectively.

In our study, the available information is not sufficient to define the complete relationship between temperature and metabolic performances, and the temperature correction factor (*TC*) is only calculated using one of the five Arrhenius parameter T_A (in K), following the equation $\tau(T) = \tau^* \exp(T_A/T_{ref} - T_A/T)$ with τa given metabolic rate, T_{ref} the reference temperature (293 $K \approx 20$ °C), T the environmental temperature (in Kelvin) and $\exp((T_A/T_{ref} - T_A/T)$ being the temperature correction factor *TC*. The correction is applied to the metabolic rates $\dot{v}$, $\dot{k}_M$, $\dot{k}_J$, $\ddot{h}_a$ (Table 1).

Temperatures recorded since 1993 at Port aux Français, another site in the Gulf of Morbihan, show a clear 6-year cycle of increasing and decreasing temperatures (Appendix A). The [2012–2018] temperature dataset selected as input forcing variable in the model therefore constitutes an interesting proxy of temperature conditions at Anse du Halage which includes a complete overview of the environmental variability at the station. However, it is important to take this choice into consideration during interpretation of results, as it needs to be differentiated from a cycle that would be inherent to the biology of the species.

2.6.2. Food resources

In DEB theory, the energy is supplied to the reserve of the organism through ingestion proportional to food availability, represented in the model by a functional response *f* (from 0 to 1). Food assimilation ($\dot{p}_A$, Fig. 3A) is proportional to the surface of the structure of each individual and contributes to the filling of the reserve compartment *E* (Fig. 3A). The functional response *f* was calibrated using the values of organic carbon (OC) content in sediment as a percentage of dry weight of sediment at the station Anse du Halage at the end of each month, available in Delille and Bouvy (1989). The maximum value of 1 for *f* corresponds here to the maximum value of organic carbon content that was found (6.94%) and a *f* minimum of 0 corresponds to 0% OC.

2.7. Model projection

2.7.1. Present-day conditions at anse du halage

To assess the influence of varying environmental conditions on model outputs, after being constructed for the site Anse du Halage, the model was implemented in two other sites, Ile Haute and Port Couvreux, where *A. cordatus* is reported in high densities (Poulin, 1996) (Fig. 1). The implementation to these two other stations was done with contrasting temperatures (from the Proteker programme, as previously explained in 2.1). Food conditions at these two sites are not available and were estimated at the end of the summer to be 50% to 30% of the organic carbon values measured at Anse du Halage according to the

comparative study of Delille et al. (1979). These rates were applied to yearlong conditions (Fig. A.2). Models were launched for a period of 200 years.

2.7.2. Future conditions

Two future scenarios predicting environmental conditions for 2100 were used, based on the IPCC scenario RCP 2.6 and 8.5 (respectively optimistic and pessimistic scenarios, IPCC 5th report), accessed at https://www.esrl.noaa.gov/psd/ipcc/ocn/ (in August 2019). Coarse IPCC predictions (1°x1° resolution) of chlorophyll a concentration were used to roughly evaluate potential changes of food availability on the east coast of the Kerguelen Island in future conditions. Scenario RCP 2.6 shows an average decrease of 10% of current food resources availability, while scenario RCP 8.5 shows an average decrease of 20% (Fig. D.3). As for temperature, we defined RCP 2.6 with a linear increase of +1.1 °C and +1.7 °C for RCP 8.5. Models were launched for a period of 30 years.

3. Results

3.1. The individual-based model

Variations in energy allocated to the reserve and the maturation buffer are the main controls of individual development. Monthly variations (∂U_E and ∂U_R, ∂X here stands for $\frac{dX}{dt}$) were simulated over one year under present-day environmental conditions (Fig. 4). Energy in the reserve (Fig. 4a) shows variations between −2.5 and 8 on average (no unit), with maximum range values reaching −5.8 and 13.7. This shows a relative constant energy density inside the reserve throughout the year with, however, a noticeable increase from October to December and a sharp decrease from December to January (Fig. 4a). According to DEB theory (Kooijman, 2010), the more energy is stored inside the reserve (through food assimilation), the more it can be distributed to other compartments, and the more energy can be assimilated into the reserve anew. Availability of food resources for *A. cordatus*is the highest in December ($f = 1$) (Fig A.2), it is assimilated and stored as energy into the reserve. Based on the energy available in the reserve at the end of December, energy is supplied in January to other compartments (such as the reproduction buffer, Fig. 4b and growth, Fig. Fa), while the individual ingests the food available to replenish its reserve anew. As food availability decreases in January ($f = 0.748$), the reserve loses energy (Fig. 4a) because the individual cannot assimilate as much energy as the amount transferred to other compartments.

The energy density entering the reproduction buffer (Fig. 4b) of mature females varies between 0 and 4.9 on average in the course of the year, with a maximum of 10.7. The rate of energy input increases at an average pace of +1.1% per month from October to the onset of the reproduction period in March, when it decreases and remains null until the end of the spawning period in June. Then, energy starts accumulating again until the next reproduction period. During the three months of the spawning period, from March to May, no energy is allocated from the reserve to the reproduction buffer and the energy stored in this buffer is progressively delivered to gametes. Only females that are mature in March undergo reproduction and deliver the energy contained in the reproductive buffer to the gametes. Females that become mature during the reproduction period undergo a normal increase of the energy in the reproduction buffer, which explains the small increasing trend observed during the March-May period (Fig. 4b).

3.2. The population model

3.2.1. Modelled population dynamics at the calibration site

Based on the individual model, population dynamics were simulated over a time period of 30 years, showing a constant population density comprised between 120 and 220 individuals per square metre. Overall, the population structure remains constant through time but with well-marked yearly variations, mainly in juvenile density (Fig. 5). Juveniles indeed represent around 83% of the total population density and show important yearly variations due to (1) important seasonal reproductive outputs causing a surge in population density, (2) strong mortality rates causing gradual decreases in the population, (3) the transfer of the large juvenile cohort to the adult population after around 3 years, and (4) the influence of inter-individual competition for food limiting population densities and even causing its decrease. In contrast, the adult population is much more stable relative to the juvenile one, with lower density values (around 40 individuals per square metre). Both juvenile and adult population fluctuations follow a general 6-year pattern displayed over the 30 years of simulations (rectangle, Fig. 5). This pattern is linked to temperature cycles over the same time span and includes two sharp decline in population density over a 6-year cycle ('T' symbol, Fig. 5), which corresponds to high temperatures rising above +8 °C during two consecutive months and causing mortality rates of 10% of the entire population.

3.2.2. Sensitivity analysis

Different parameter settings for the model initiation may result in very diverging outputs (Appendix E). It also influences model stability,

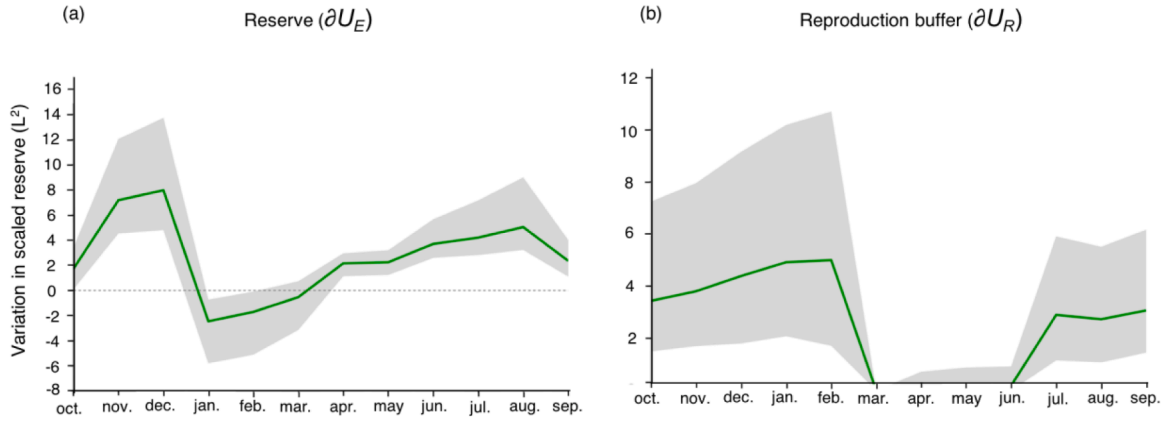

Fig. 4. Simulation of the variation of energy allocated to the reserve (a) and the reproduction buffer (b) compartments over one year. Males were not considered in the model when simulating reproduction processes, and thus results presented here only take females into consideration. Average results for all mature females, in 100 model simulations are presented by the green line. The grey area corresponds to the variation range (variation induced by differences between individuals: age, size, energy allocation) between all females amongst the 120 individuals that initiate the model. The variation in energy allocated is the change in a scaled variable X: ∂X here stands for $\frac{dX}{dt}$(for an explanation of the term "scaled" here, see Section 2.4.2). (For interpretation of the references to colour in this figure legend, the reader is referred to the web version of this article.)

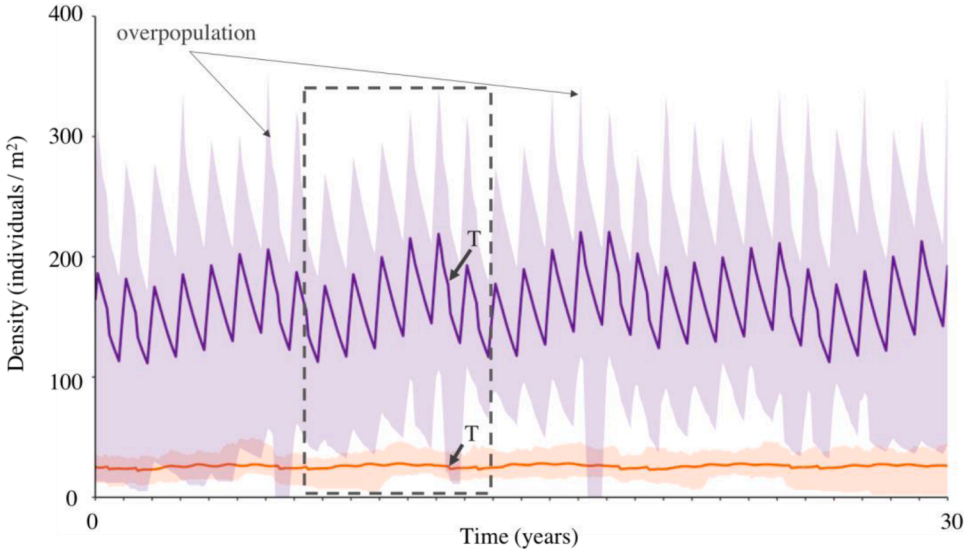

Fig. 5. Modelled population structure and density under present-day environmental conditions: monthly values of juvenile density (purple) and adult density (orange) over 30 years (for 100 simulations). Bold lines: mean density value. Shaded areas: variation range for the 100 simulations. 'T' symbol: sharp decrease in population density due to temperature-induced mortality. Dashed-line rectangle: 6-year cycle in population dynamics (this 6-year pattern is due to the input temperature data and not to a biological cycle inherent to the population). (For interpretation of the references to colour in this figure legend, the reader is referred to the web version of this article.)

and population collapse in particular. Overall, the initial number of individuals and the level of the inter-individual variation coefficient are parameters that have little influence on model stability and low proportion of population crashes may result. In addition, model outputs do not differ significantly between simulations. Increase in juvenile and adult mortality levels will also have little influence on model outputs but decreasing mortality levels will induce a population burst followed by a strong competition for food and a consequent population collapse. amongst all the parameters set at the model initialisation, egg number and egg survival are the most important determining model stability, as they directly control juvenile density. High juvenile densities (induced by a low background juvenile mortality and a high number of eggs and egg survival) always result in fast population collapses as a result of high competition for food between individuals. As population density increases, the amount of food available for each individual decreases and individuals start starving to death. In contrast, a reduction in the number of juveniles causes a reduction in the average population density due to a strong mortality rate of juveniles. It does not imply model instability and the proportion of modelled population crashes is always lower than 15%. The reduction of population density also strongly influences the average amount of energy available for each individual: the more energy is available, the more individuals can grow in structural length.

3.2.3. *Projections of the population dynamics model to other sites*

The dynamic population model built at Anse du Halage was implemented (Appendix G) for the two sites of Ile Haute (inside the Morbihan Bay) and Port Couvreux (outside the Morbihan Bay). Both models were simulated twice with initial estimates of 50% and 30% of food availability (f) compared to Anse du Halage (f_H). Temperature inputs were based on local temperature variations recorded at the two sites. Model outputs predict lower population densities at both sites compared to Anse du Halage and interestingly, similar ratios between juveniles and adults (Table 4). These results are consistent with density values found in the literature, which give between 100 and 136 individuals/m^2 at Ile Haute and 50 to 168 ind./m^2 at Port Couvreux (Mespoulhé, 1992; Poulin, 1996). The different observed density values reported in publications for Port Couvreux may be due to contrasting conditions that locally prevail amongst the three small embayments of that locality (Poulin, 1996). This has recently been confirmed by our personal observations in the field (Saucède, 2020). Model outputs suggest a strong influence of food availability on population densities controlled by inter-individual competition for food. Accordingly, simulations predict a drop in density values at Port Couvreux when food resources decrease at 30% of f_H, while density values are relatively stable at Ile Haute in comparison (Table 4a). This mainly affects juvenile densities and results in a lower population ratio (Table 4b).

Table 4
Modelled population densities (a) and juveniles over adults ratio (b) at the calibration (Anse du Halage) and projection (Ile Haute and Port Couvreux) sites. Average and standard deviation values are given for 100 model replicates and 200 years of simulation. f_H: time series of f value at Anse du Halage (Delille and Bouvy 1989).

(a)	Anse du Halage	Ile Haute	Port Couvreux
f_H, T°Halage	182.6 ± 49	–	–
50% of f_H, T°site	–	137.6 ± 40	137.4 ± 41
30% of f_H, T°site	–	123.2 ± 38	91.8 ± 44
(b)	Anse du Halage	Ile Haute	Port Couvreux
f_H, T°Halage	6.53 ± 3.12	–	–
50% of f_H, T°site	–	6.31 ± 4.40	6.32 ± 4.31
30% of f_H, T°site	–	6.04 ± 4.31	3.87 ± 2.61

Temperatures recorded at the two sites inside the Morbihan Bay (Anse du Halage and Ile Haute) are close to each other and slightly higher than outside the Bay at Port Couvreux (Fig. A.1). Contrasting results were therefore expected between Port Couvreux and the two other sites. On the contrary, temperatures may not be contrasting enough between sites to affect population structure and density. Confidence intervals overlap between all sites for values of both population density and juveniles-adults ratio (Table 4).

3.2.4. *Population dynamics under future predictions of climate change*

Population structure and density were simulated and implemented for scenarios of temperature and food resources changes based on IPCC scenarios RCP 2.6 and 8.5, and for populations of 'resistant', 'intermediate' and 'vulnerable' organisms (Fig. 6). Population dynamics are all predicted to be affected by both scenarios (Fig. 6d, 6g) with overall population densities predicted to be four to seven times lower than current population predictions. Population structures are also predicted to be affected by a lower contribution of juveniles to overall population densities. The respective effects of temperature (Fig. 6b) and resource availability (Fig. 6c) were simulated independently. Under temperature change only (Fig. 6b), model predictions are close to model outputs in which both variables are combined (Fig. 6g), with a strong decrease in average population density compared to present-day conditions (Fig. 6a). The effect of changes in resources availability only (Fig. 6c) is less marked, with population densities showing a close pattern to present-day models (Fig. 6a).

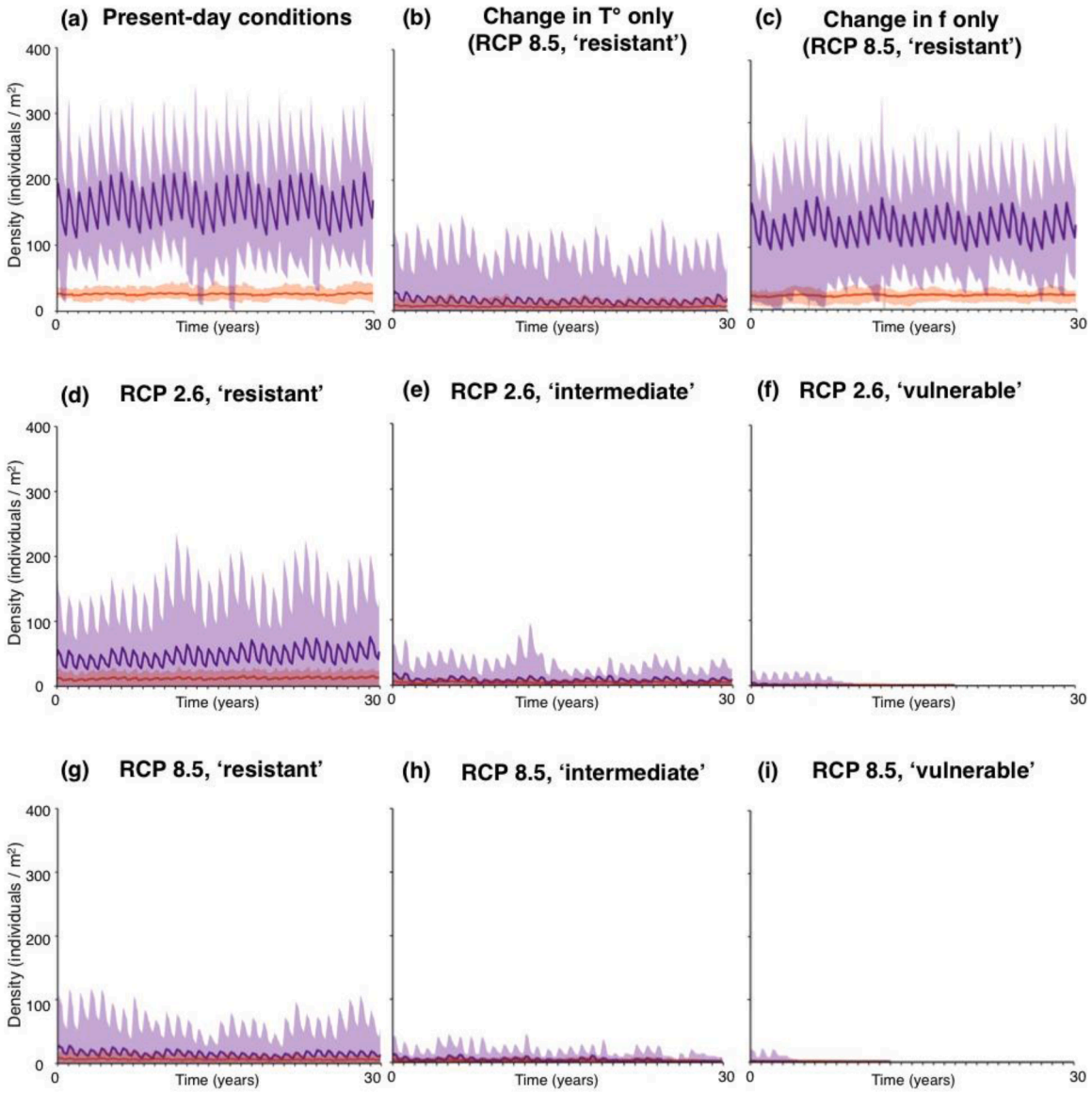

Fig. 6. Model predictions under IPCC scenarios RCP 2.6 and RCP 8.5 of environmental change (for 100 simulations). Purple: adult population, orange: juvenile population. Coloured bold lines show mean values for 100 simulations. Shaded areas are simulation variation ranges. (a) Population model under present-day conditions, (b) model under IPCC scenario RCP 8.5 of T° change only (+1.7 °C compared to present) and for resistant organisms; (c) model under IPCC scenario RCP 8.5 of *f* change only (−20% compared to present) and for resistant organisms; (d) model under IPCC scenario RCP 2.6 of T° and *f* changes (−10% of *f* and +1.1 °C compared to present) and for 'resistant' organisms; (e) model under IPCC scenario RCP 2.6 of T° and *f* changes and for 'intermediate' organisms; (f) model under IPCC scenario RCP 2.6 of T° and *f* changes and for 'vulnerable' organisms; (g) model under IPCC scenario RCP 8.5 of T° and *f* changes and for 'resistant' organisms; (h) model under IPCC scenario RCP 8.5 of T° and *f* changes and for 'intermediate' organisms; (i) model under IPCC scenario RCP 8.5 of T° and *f* changes and for 'vulnerable' organisms. (For interpretation of the references to colour in this figure legend, the reader is referred to the web version of this article.)

Models therefore predict a stronger effect of temperature changes on populations, with population densities of 'vulnerable' organisms predicted as very low (less than one tenth of present-day densities on average). Populations of 'vulnerable' organisms are even predicted to go extinct in only 30 years of simulation (Fig. 6f, 6i). Populations of organisms with 'intermediate' sensitivity (Fig. 6e, 6h) are more resilient and withstand over 30 years of simulation in some cases, but they collapse at the end of the period under IPCC scenario RCP 8.5. Overall densities are very low (around 20 or less individuals per square metre on average).

3.3. Population mortality under present-day and future predictions

Under present-day conditions (Fig. 7b), background mortality and ageing are the main causes that affect population mortality each year (respectively 65 to 90%% and 5.8 to 9%). High temperatures and starvation have sporadic effects on mortality. High mortality due to high temperatures only happened in [2016–2017] and [2017–2018] and starvation contributes at the highest to 10% of overall mortality, depending on the year.

Over the course of a year (Fig. 7a), background mortality and ageing affect the population every month, while high temperatures (over 8 °C) cause the death of half of the population in March and April. Starvation is responsible for the death of a weak proportion of the population in November and December only (austral summer), in link with the competition for food resources of the increasing population during this productive and warm period.

Under both future scenarios (Fig. 7e, 7f), mortality levels are low compared to present-day model (Fig. 7b), which is mostly due to small predicted population densities. Background and ageing mortalities are

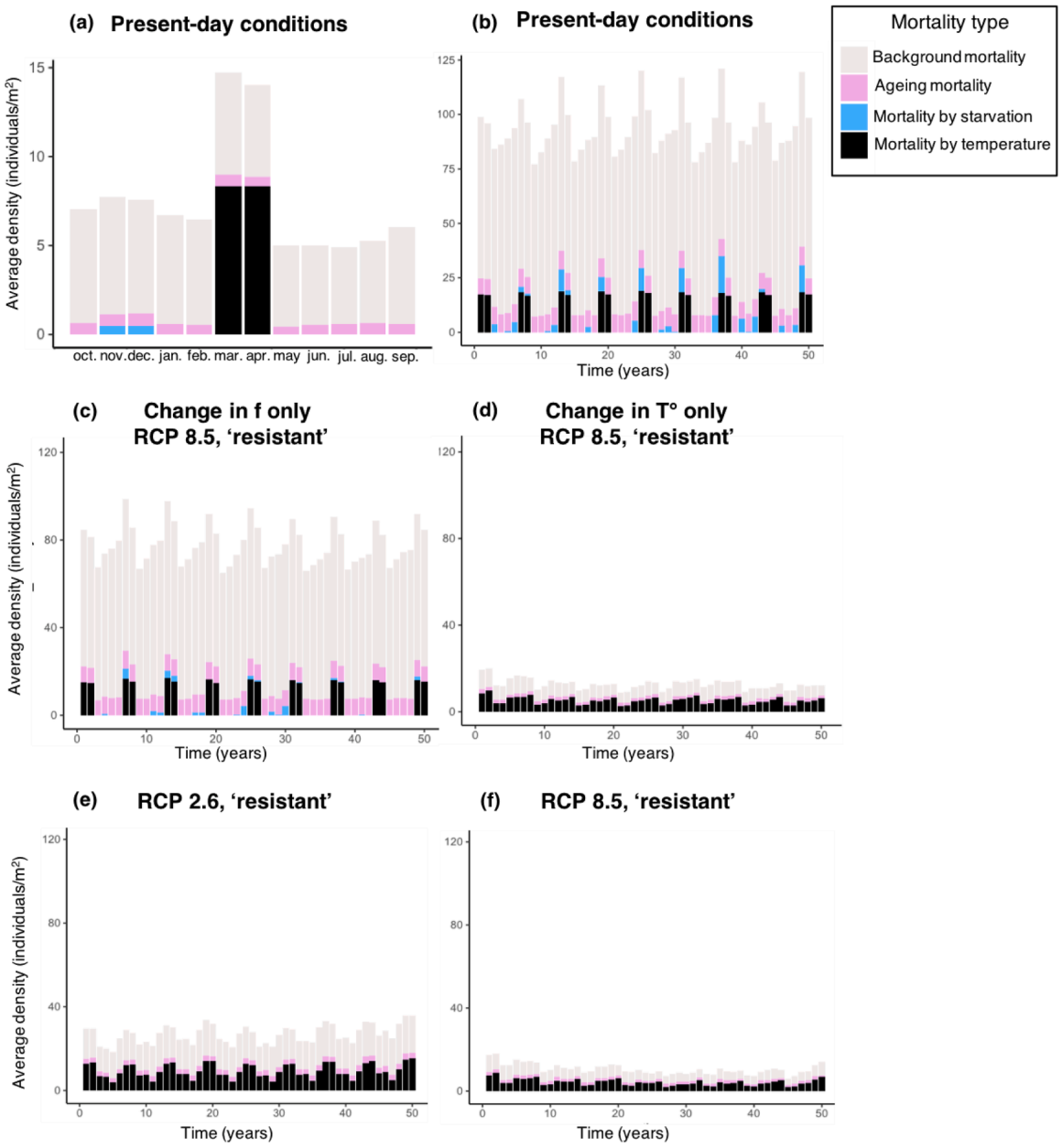

Fig. 7. Mortality simulations (in individuals/m^2) per month (7a) and year (7b-f) under present-day (7a-b) and future (7c-f) predictions of the two IPCC scenarios (for 100 model simulations). (a) Model under present-day conditions for 12 months (year #7 [2016–2017] was chosen as an example); (b) Model under present-day conditions for 50 years of simulations; (c) Simulated mortality under scenario RCP 8.5 for resistant organisms and predicted changes in food availability only (f=−20% compared to present); (d) Simulated mortality under scenario RCP 8.5 for resistant organisms and predicted changes in temperature only (+1.7 °C compared to present); (e) Simulated mortality under scenario RCP 2.6 for resistant organisms and predicted changes in both food availability and temperature (food reduction of −10%, T° increase of +1.1 °C); (f) Simulated mortality under scenario RCP 8.5 for resistant organisms and predicted changes in food availability and temperature (food reduction of −20%, T° increase of +1.7 °C). (For interpretation of the references to colour in this figure legend, the reader is referred to the web version of this article.)

therefore very low. Starvation is not a cause of mortality anymore, while high temperatures cause mortality of individuals before they may starve to death. When comparing between model predictions under scenario RCP 8.5 for changes in food availability only (Fig. 7c), temperature change only (Fig. 7d), and the combined variables (Fig. 7f), temperature clearly appears as the main cause of mortality, at the same level as background mortality.

4. Discussion

4.1. Potential and limitations of the DEB-IBM approach

In the present work, a DEB-IBM model was built for *A. cordatus* based on our current knowledge of this vulnerable, endemic species of the Kerguelen plateau. On-site monitoring and experiments on species tolerance to changing environmental conditions remains challenging issues in the Kerguelen Islands, and in the Southern Ocean in general.

Difficulties are owed to the sensitivity of specimens (Magniez, 1983; Schatt, 1985; Mespoulhé, 1992) and the inherent ecological characteristics. Models can constitute a powerful tool for Antarctic research as they can provide additional support to experimental knowledge and infer the impact of broad-scale climate change on populations. The potential of the present mechanistic modelling approach resides in its capacity to model the physiology of organisms as a response to environmental factors. Using DEB models for the representation of individual components within the IBM enables to upscale a dynamic model to an entire population (Railsback and Grimm 2019) as a function of two changing abiotic factors: temperature and food resources. Applying such a model to a sub-Antarctic, benthic, and brooding species is challenging, and had never been performed so far. The present work shows the feasibility and relevance of the DEB-IBM approach to study Southern Ocean species like *A. cordatus*.

Relevant results were obtained both at the individual and populations levels. First, simulations showed the characteristic annual evolution of energy dynamics in the organism (Fig. 4, Appendix F) and second, population structure and density dynamics were modelled over an extended period of time decoupling juvenile and adult populations (Table 4, Fig. 6, Fig. 7). Projections to other sites also show the potential application of the model to other areas for which environmental data are available. Future models give an insight and add some clues to assess the potential impact of climate change and predict the biotic response of populations. Models however still need some improvements including complementary data on species ecophysiology. The model was also shown to be sensitive to mortality rates and some parameters (egg number and egg survival) settings while some population characteristics (initial population densities and inter-individual variability) have little effects (Appendix E).

4.2. Limitations to the DEB-individual model

The dynamic population model built in this work uses outputs from the DEB model developed for *A. cordatus* (Guillaumot, 2019), which allows to represent as faithfully as possible the physiological dynamics of individuals during their entire life cycle. The goodness of fit of the DEB model shows that estimated parameters accurately described observed data. However, collecting additional data at the different stages of the organism's life cycle and under different conditions of temperature and food availability would contribute to improving further model accuracy and parameter predictions. In particular, data on environmental settings and species ecophysiology are still needed to improve the accuracy and relevance of the following parameters.

4.2.1. The arrhenius function and the optimal temperature range

In DEB theory, the Arrhenius function determines the optimal temperature range of the organism's metabolism as a response to enzymatic tolerance (Kooijman, 2010; Thomas and Bacher 2018). In the present work, calculation of the Arrhenius function relies on fragmental datasets. The ascending part of the Arrhenius curve that is, the temperature range in which faster metabolic rates are determined by higher temperatures was estimated, but values are still missing for the descending slope (i.e. the temperature range beyond the optimal temperatures in which the metabolic rates slow down with higher temperatures) (Kooijman, 2010). The present model assumes that higher temperatures favour more suitable conditions with no limit (Appendix F), which has to be corrected arbitrarily using our personal field and experimental observations on the echinoid ecology (Fig. D.2). Further experiments should help improve the calculation of the Arrhenius function. They would consist in measurements of respiratory rates as a function of temperature variations (e.g. Uthicke et al., 2014) and will enable more accurate simulations of *A. cordatus*' ecophysiology and the direct effect of temperature on the organism's metabolism, a prerequisite to better model population mortality.

4.2.2. Age, size, and growth estimates

Most parameters used in the DEB model were taken from the literature and experimental studies, except for some of them that were assumed based on physiological traits of counterparts. In particular, organisms' maximum age, growth rate and size are not sufficiently known due to difficulties in setting up long-term experiments in the Kerguelen Islands. The relationship between echinoid growth, size and shape cannot be assessed based on growth lines measurement because there is no linear relationship between echinoid size and age (Ebert, 1975) and because resorption may occur during periods of starvation (Brockington et al., 2001; Ingels et al., 2012). The most reliable method would consist in monitoring organisms' growth through time using tagging methods (Ebert, 2013). However, such an approach is time-consuming and challenging as even small measurement errors may have a significant effect on results (Ebert, 2013) and no experimental data are available so far.

Former studies (Mespoulhé, 1992) showed that after 4 to 5 years, specimens of *A. cordatus* only slowly increase in size and echinoids' test tend to become distorted, a common feature in large spatangoid echinoids in which test plates tend to overlap while body size does not increase anymore (Mespoulhé, 1992). However, this slow growth rate in aged specimens could also result from other causes affecting optimal food intake for instance. At the calibration site of Anse du Halage, a study of echinoid cohorts suggests that few individuals grow older than six years old (Poulin and Féral 1994). Overall, the absence or nearly absence of growth in old invertebrate organisms makes age estimates delicate to assess. In the present model, based on the combination of the ageing sub-model and other mortality processes, most individuals are calibrated to die within the assumed maximum age (before 6 years old), although some individuals may reach over ten years old due to the chosen stochasticity introduced in the sub-model.

Juveniles inside brood pouches were assumed to grow at a constant and same rate as adults but it has sometimes been assumed that the brooded young may already feed and develop at a faster rate (Schatt, 1985; Schatt and Féral 1996). At this stage, the offspring is particularly fragile and needs protection in the brood pouches to survive, which prevents any monitoring of growth rates and feeding behaviours (Magniez, 1983; Schatt, 1985; Mespoulhé, 1992).

4.3. Ecological relevance of the IBM population model

Upscaling the DEB-individual model to the population level in the IBM enables to simulate population structure and dynamics as a response to temperature and food resource availability. In particular, the IBM enables to predict the targetted effect of environmental changes on the population at the different life stages of individuals. Additional environmental data would help enhance IBM reliability and improve our knowledge of populations and environmental conditions in remote areas.

Field works are also subject to uncertainties due to the species burrowing habit which renders the assessment of population structure difficult, the brittleness of specimens also limiting counting replicates (Magniez, 1980; Mespoulhé, 1992). Important variations in population densities were noted across studies (Guille and Lasserre 1979; Mespoulhé, 1992; Poulin, 1996, personal observations) for a same site, which may suggest either important variations in population density and structure through time, which was however refuted by Poulin and Féral (1994), or important biases in sampling due to the aggregative behaviour of individuals and the patchiness of distribution patterns (Poulin, 1996).

The sensitivity analysis (Appendix E) showed that the model is not very much dependant on assumptions made on initial population densities because the model density-dependant regulation operates through intra-specific competition for food resources only. There is no agonistic behaviour amongst conspecific individuals as it was reported in other echinoid species (e.g. *Echinometra* sp. Shulman, 1990) and there is no

evidence of competition for space in *A. cordatus* based on field observation. Intra-specific competition in shallow-water echinoids is a common phenomenon under food-limited conditions (Stevenson, Mitchell, and Davies, 2015). McClanahan and Kurtis (1991) stated that in *Echinometra mathaei*, when predation pressure and intra-specific competition are low, populations increase without limitation and regulation operates through a decrease in food availability for individuals. The same could hold true for *A. cordatus* as well.

Intra-specific competition for oxygen could also have a regulatory effect (Ferguson et al., 2013) since *A. cordatus* shows a high oxygen consumption rate (Guille and Lasserre 1979; Magniez and Féral 1988). In muddy substrates, specimens are usually observed unburied, positioned onto the sediment (instead of underneath), which was often interpreted as a result of difficulties to breath inside fine sediments.

The sensitivity analysis also showed that the number of eggs produced by females is a controlling parameter of model stability as well. There is a high variability in the number of eggs produced amongst females (from 9 to 106 eggs per female, personal communication from P. Magniez). Taking into account such a variability would introduce an enhanced stochasticity in the population dynamics model if implemented and linked to each female's reproductive buffer U_R and GSI values (Martin et al., 2010, e.g. for zebrafish in Beaudouin et al., 2015).

Finally, the model was also shown to be sensitive to background mortality (Appendix E). Although monitoring mortality rates in the field is challenging, such data would greatly enhance the reliability of the IBM.

In general, the sensitivity tests showed that the model works with the current quality and quantity of data available for this species in this habitat. However, on the matter of the temporal resolution, our model needs to be expanded and further consolidated, and we consider this element as a limitation to our work in its current state (Appendix C).

4.3.1. Modelled food resources

The organic content of sediments is one of the main food resources for detritus feeders and sediment swallowers like *A. cordatus* (Snelgrove and Butman 1994) and Antarctic echinoids (Michel et al., 2016). In the present model, the organic carbon content of sediments was used as a proxy for food availability for *A. cordatus*. Intra-specific competition for food has a stronger effect on resources availability than seasonal variations in resource availability. This is in line with ecological evidences that populations of *A. cordatus* survive periods of low food resources that prevail during the austral winter. High seasonality in food resources is a common feature of polar ecosystems and species have long adapted their diet accordingly (De Ridder and Lawrence 1982; Michel et al., 2016). This has been shown in Antarctic benthic invertebrates such as shallow-water brachiopods (Peck et al., 2005), cnidarians (Orejas et al., 2001), and echinoids (Brockington et al., 2001; Ingels et al., 2012). For instance, the Antarctic sea urchin *Sterechinus neumayeri* is believed to be capable of mobilizing energy from gut tissues, gonads and the body wall during the austral winter (Brockington et al., 2001), a strategy that may have been evolved in *A. cordatus* as well (Magniez, 1983). Shrinking and resorption, which are sometimes hypothesized as a survival mechanism in other echinoids facing long periods of starvation, are phenomena which are still understudied (David and Néraudeau 1989; Ebert, 2013) and have not been verified in *A. cordatus*. In the present model, starvation results in the redirection of the energy flow exclusively toward maintenance of structure, at the expense of other compartments. Although Magniez (1983) observed a decrease in gonadal material after the reproduction period, it is very small in females (- 0.3%) and slightly bigger in males (−1.6%), and the exact cause has not been studied. It is not known whether this decrease in gonadal material can be directly attributed to a reabsorption for survival purposes or some other mechanism. The use of previously stored energy in the different compartments to sustain the maintenance of structure is assumed to be non-existent in our model. Such starvation processes could be tested in future implementation, provided sufficient data is obtained through experimental setups observing the phenomenon.

The two scenarios of future food availability were based on coarse IPCC and NOAA projection models for the region. These simulations and associated outputs are here considered as conceivable scenarios of the influence of food and temperature changes on population dynamics. They are used as a proof of concept and are by no means considered as definite and reliable scenarios of population dynamics in the future. Future accurate predictions should imply the integration of complex mechanisms influencing the production, transport and deposition of organic matter in the ocean, the possibility of species to adapt to changing environmental conditions, and more experimental data are needed to integrate the detailed influence of temperature on physiological processes. First observations suggest a low response toward the applied changes in food availability, in comparison with the influence of temperature. However, it cannot be concluded that the species would not be affected by future conditions in food resources in the area.

4.3.2. Temperature resilience

Important differences were obtained between population structures and densities depending on future scenarios and model projections made for contrasting food resources and temperature. Most importantly, the 'resistant' population model of *A. cordatus* at Anse du Halage is predicted to sustain the expected changes in temperature and food resources under both future scenarios although population density is also predicted to be strongly reduced. In contrast, the 'vulnerable' population model predicts population extinction after a few decades of simulation. This implies that a precise evaluation of the species resilience to temperatures is needed for more robust and decisive models. Moreover, Antarctic echinoids were shown to present varied responses to ocean warming depending on species and life stages, with higher vulnerability to warm temperatures in juveniles than in adults (Ingels et al., 2012). Such a contrast suggests that more data could help fine-tune the present model.

4.4. Relevance of the DEB-IBM approach for southern ocean studies

DEB-IBM models are being developed for various applications and research fields. They are considered a powerful tool for environmental risk assessment, such as the effect of toxicity (e.g. Beaudouin et al., 2015, David et al., 2019; Vlaeminck et al., 2019,) and the impact of environmental changes on population dynamics (e.g. Malishev et al., 2018; Saraiva et al., 2014 , , Thomas and Bacher 2018, Goedegebuure et al., 2018). They can also be used to predict the behaviour of microbial systems (Jayathilake et al., 2017) or bring to light underlying mechanisms of life history strategies (e.g. Gatti, Petitgas, and Huret, 2017). The DEB model brings ontogenetic and phenotypic variations to the population model while the IBM brings stochasticity, population dynamics (e.g. competition for food), as well as learning and interaction mechanisms (DeAngelis et al., 1991; Martin et al., 2012;) to complement the model. The potential of the DEB-IBM approach resides in the combination of both models to predict population dynamics as a response to changing environmental conditions (i.e. at the individual level in the DEB model and at population level in the IBM)

In the present work, the DEB-IBM was used to improve our understanding of the dynamics of *A. cordatus'* populations. Applications could be further developed to address conservation issues such as the designation of priority areas and the definition of management plan strategies. Vast areas of the French Southern Territories have recently been placed under enhanced protection of a national nature reserve based on experts' knowledge and ecoregionalisation approaches (Koubbi et al., 2010; Fabri-Ruiz et al., 2020). Most areas however could not have benefited from thorough benthic field studies, and ecological models can represent interesting tools to assess the relevance of defined protection areas for target species and ecosystems. Such models can be useful when drafting management plan strategies for determining favored ship traffic routes or areas where human activities can be implemented in coastal areas of the national nature reserve of the French Southern Territories.

Dynamic population models allow testing different ecological scenarios in a quite straightforward way to illustrate research designs and proposals. They can provide some clues to investigate the potential effect of environmental changes on key species for which conservation efforts should be directed in a short to long-term strategy (Fulton et al., 2015). Dynamic models can also prove useful for adaptable conservation strategies like the designation of dynamic protected areas as a consequence of changing environments and ecosystems. Finally, dynamic models could be further implemented into studies of ecosystem functioning and the impact of environmental changes on the alteration of sub-Antarctic ecosystems.

Declaration of Competing Interest

The authors declare that they have no known competing financial interests or personal relationships that could have appeared to influence the work reported in this paper.

Acknowledgements

The authors would like to thank Yoann Thomas and Cédric Bacher for their valuable advice during model construction, and Pierre Magniez for his contribution with data on *A. cordatus* reproduction strategies. The present work is a contribution to the IPEV programme PROTEKER (No. 1044) and the French LTER Zone ATelier Antarctique (ZATA). It is also contribution no. 39 to the vERSO project (www.versoproject.be), funded by the Belgian Science Policy Office (BELSPO, contract n°BR/132/A1/vERSO) and contribution no. 13 to the "Refugia and Ecosystem Tolerance in the Southern Ocean" project (RECTO; BR/154/A1/RECTO) funded by the Belgian Science Policy Office (BELSPO). M A-P was supported by the French Foundation for Research on Biodiversity and its partners (FRB - www.fondationbiodiversite.fr). This work was supported by a "Fonds pour la formation à la Recherche dans l'Industrie et l'Agriculture" (FRIA) and « Bourse fondation de la mer » grants to CG.

Supplementary materials

Supplementary material associated with this article can be found, in the online version, at doi:10.1016/j.ecolmodel.2020.109352.

References

Agassiz, A., 1881. Report on the Echinoidea dredged by H.M.S. Challenger during the years 1873–1876. Report on the scientific results of the voyage of H.M.S. Challenger during the years 1873–1876. Zoology 3, 1–321.

Améziane, N., Eléaume, M., Hemery, L., Monniot, F., Hemery, A., Hautecoeur, M., Dettai, A., 2011. Biodiversity of the Benthos off Kerguelen Islands: overview and Perspectives. In: Duhamel, G., Welsford, D. (Eds.), The Kerguelen Plateau, marine ecosystem and fisheries. Société Française d'Ichtyologie, pp. 157–167.

Arnaud, P.M., 1974. Contribution a la bionomie benthique antarctique et subantarctique. Ph. D. Dissertation, Station marine d'Endoume, Marseille.

Beaudouin, R., Goussen, B., Piccini, B., Augustine, S., Devillers, J., Brion, F., Péry, A.R., 2015. An individual-based model of zebrafish population dynamics accounting for energy dynamics. PLoS ONE 10 (5), e0125841. https://doi.org/10.1371/journal.pone.0125841.

Brockington, S., Clarke, A., Chapman, A., 2001. Seasonality of feeding and nutritional status during the austral winter in the antarctic sea urchin *Sterechinus neumayeri*. Mar. Biol. 139, 127–138. https://doi.org/10.1007/s002270100561.

Constable, A.J., Melbourne-Thomas, J., Corney, S.P., Arrigo, K.R., Barbraud, C., Barnes, D.K., Bindoff, N.L., Boyd, P.W., Brandt, A., Costa, D.P., 2014. Climate change and Southern Ocean ecosystems I: how changes in physical habitats directly affect marine biota. Glob Chang Biol 20 (10), 3004–3025. https://doi.org/10.1111/gcb.

Convey, P., Peck, L.S., 2019. Antarctic environmental change and biological response. Sci Adv 5 (11). https://doi.org/10.1126/sciadv.aaz0888 eaaz0888.

David, B., Néraudeau, D., 1989. Tubercle loss in Spatangoids (Echinodermata, Echinoides): original skeletal structures and underlying processes. Zoomorphology 109, 39–53. https://doi.org/10.1007/BF00312182.

David, B., Choné, T., Mooi, R., De Ridder, C., 2005. Antarctic Echinoidea. Synopses of the Antarctic benthos. Koeltz Scientific Books, Königstein, p. 273.

David, V., Joachim, S., Tebby, C., Porcher, J.M., Beaudouin, R., 2019. Modelling population dynamics in mesocosms using an individual-based model coupled to a bioenergetics model. Ecol Modell 398 (C), 55–66. https://doi.org/10.1016/j.ecolmodel.2019.02.008.

DeAngelis, D.L., Godbout, L., Shuter, B.J., 1991. An individual-based approach for predicting density-dependent dynamics in smallmouth bass populations. Ecol Modell 57, 91–115. https://doi.org/10.1016/0304-3800(91)90056-7.

DeAngelis, D.L., Mooij, W.M., 2005. Individual-based modeling of ecological and evolutionary processes. Annu Rev Ecol Evol Syst 36, 147–168. https://doi.org/10.1146/annurev.ecolsys.36.102003.152644.

Delille, D., Gadel, F., Cahet, G., 1979. La matière organique dans les dépots de l'archipel des Kerguelen. Distribution spatiale et saisonnière. Oceanologica acta 2 (2), 181–193.

Delille, D., Bouvy, M., 1989. Bacterial responses to natural organic inputs in a marine subantarctic area. Hydrobiologia 182 (3), 225–238. https://doi.org/10.1007/BF00007517.

De Ridder, C., Lawrence, J.M., 1982. Food and feeding mechanisms: echinoidea. In: Jangoux, M., Mawrence, J.M. (Eds.), Echinoderm nutrition. A.A. Balkema Publisheres, Rotterdam, pp. 57–115.

De Ridder, C., David, B., Larrain, A., 1992. Antarctic and Subantarctic echinoids from "Marion Dufresne" expeditions MD03, MD04, MD08 and from the "Polarstern" expedition Epos III. Bulletin du Muséum national d'histoire naturelle. Section A. Zoologie, biologie et écologie animales 14 (2), 405–441.

Ebert, T.A., 1975. Growth and mortality of post-larval echinoids. Integr. Comp. Biol. 15 (3), 755–775. https://doi.org/10.1093/icb/15.3.755.

Ebert, T.A., 2013. Growth and survival of postsettlement sea urchins. In: lawrence (Ed.), Sea Urchins: Biology and Ecology. Developments in Aquaculture and Fisheries Science, pp. 83–117. https://doi.org/10.1016/B978-0-12-396491-5.00007-1.

Fabri-Ruiz, S., Danis, B., Navarro, N., Koubbi, P., Laffont, R., Saucède, T., 2020. Benthic Ecoregionalization based on echinoid fauna of the Southern Ocean supports current proposals of Antarctic Marine Protected Areas under IPCC scenarios of climate change. Glob Chang Biol.

Fenaux, L., Malara, G., Charra, R., 1975. Effets d'un jeûne de courte durée sur les principaux constituants biochimiques de l'oursin *Arbacia lixula*. I. Stade de repos sexuel. Mar. Biol. 30 (3), 239–244. https://doi.org/10.1007/BF00390746.

Féral, J.P., .& Magniez, P., 1988. Relationship between rates of oxygen consumption and somatic and gonadal size in the subantarctic echinoid Abatus cordatus from Kerguelen. In 6th International Echinoderm Congress (pp. 581–587).

Féral, J.P., Poulin, E., González-Wevar, C.A., Améziane, N., Guillaumot, C., Develay, E., Saucède, T., 2019. Long-term monitoring of coastal benthic habitats in the Kerguelen Islands: a legacy of decades of marine biology research. In: Welsford, D., Dell, J., Duhamel, G. (Eds.), The Kerguelen Plateau: Marine ecosystem and fisheries. Proceedings of the Second Symposium. Australian Antarctic Division, Kingston, Tasmania, Australia, pp. 383–402. https://doi.org/10.5281/zenodo.3249143. ISBN: 978-1-876934-30-9.

Ferguson, N., White, C., Marshall, D., 2013. Competition in benthic marine invertebrates: the unrecognized role of exploitative competition for oxygen. Ecology 94, 126–135. https://doi.org/10.2307/23435675.

Fulton, E.A., Bax, N.J., Bustamante, R.H., Dambacher, J.M., Dichmont, C., Dunstan, P.K., Hayes, K.R., Hobday, A.J., Pitcher, R., Plagányi, E.E., 2015. Modelling marine protected areas: insights and hurdles. Philosophical Transactions of the Royal Society B 370, 1681. https://doi.org/10.1098/rstb.2014.0278.

Gatti, P., Petitgas, P., Huret, M., 2017. Comparing biological traits of anchovy and sardine in the Bay of Biscay: a modelling approach with the Dynamic Energy Budget. Ecol Modell 348, 93–109. https://doi.org/10.1016/j.ecolmodel.2016.12.018.

Goedegebuure, M., Melbourne-Thomas, J., Corney, S.P., McMahon, C.R., Hindell, M.A., 2018. Modelling Southern Elephant Seals *Mirounga leonina* using an Individual-based Model coupled with a Dynamic Energy Budget. PLoS ONE 13 (3), e0194950. https://doi.org/10.1371/journal.pone.0194950.

Grimm, V., Railsback, S.F., 2005. Individual-based modeling and ecology. Princeton university press.

Grimm, V., Berger, U., DeAngelis, D.L., Polhill, J.G., Giske, J., Railsback, S.F., 2010. The ODD protocol: a review and first update. Ecol Modell 221, 2760–2768. https://doi.org/10.1016/j.ecolmodel.2010.08.019.

Grimm, V., Berger, U., 2016. Robustness analysis: deconstructing computational models for ecological theory and applications. Ecol Modell 326, 162–167. https://doi.org/10.1016/j.ecolmodel.2015.07.018.

Guillaumot, C., Martin, A., Fabri-Ruiz, S., Eléaume, M., Saucède, T., 2016. Echinoids of the Kerguelen Plateau – occurrence data and environmental setting for past, present, and future species distribution modelling. Zookeys 630, 1–17.

Guillaumot, C., Martin, A., Eléaume, M., Saucède, T., 2018a. Methods for improving species distribution models in data-poor areas: example of sub-Antarctic benthic species on the Kerguelen Plateau. Mar. Ecol. Prog. Ser. 594, 149–164.

Guillaumot, C., Fabri-Ruiz, S., Martin, A., Eléaume, M., Danis, B., Féral, J.P., Saucède, T., 2018b. Benthic species of the Kerguelen Plateau show contrasting distribution shifts in response to environmental changes. Ecol Evol 8 (12), 6210–6225. https://doi.org/10.1002/ece3.4091.

Guillaumot, C. (2019). AmP Abatus cordatus, version 2019/01/17. https://www.bio.vu.nl/thb/deb/deblab/add_my_pet/entries_web/Abatus_cordatus/Abatus_cordatus_res.html.

Guille, A., Lasserre, P., 1979. Consommation d'oxygène de l'oursin *Abatus cordatus* (Verrill) et activité oxydative de son biotope aux îles Kerguelen. Mémoires du Muséum National d'Histoire Naturelle. Paris 43, 211–219.

Gutt, J., Isla, E., Bertler, A.N., Bodeker, G.E., Bracegirdle, T.J., Cavanagh, R.D., Comisco, J.C., Convey, P., Cummings, V., De Conto, R., et al., 2018. . Cross-disciplinarity in the advance of Antarctic ecosystem research. Mar Genomics 37, 1–17. https://doi.org/10.1016/j.margen.2017.09.006.

Hibberd, T., Moore, K., 2009. Field Identification Guide to Heard Island and McDonald Islands Benthic Invertebrates, a guide for scientific observers on board fishing vessels in that area. The Department of Environmentthe Arts. Australian Antarctic Division

and the Fisheries Research and Development Corporation, Water, Heritage, andAustralia, ISBN 978-1-876934-15-6, p. 158.
Ingels, J., Vanreusel, A., Brandt, A., Catarino, A.I., David, B., De Ridder, C., Dubois, P., Gooday, A.J., Martin, P., Pasotti, F., Robert, H., 2012. Possible effects of global environmental changes on Antarctic benthos: a synthesis across five major taxa. Ecol Evol 2 (2), 453–485. https://doi.org/10.1002/ece3.96.
Jayathilake, P.G., Gupta, P., Li, B., Madsen, C., Oyebamiji, O., González-Cabaleiro, R., Rushton, S., Bridgens, B., Swailes, D., Allen, B., et al., 2017. A mechanistic Individual-based Model of microbial communities. PLoS ONE 12 (8), e0181965. https://doi.org/10.1371/journal.pone.0181965.
Jusup, M., Sousa, T., Domingos, T., Labinac, V., Marn, N., Wang, Z., Klanjšček, T., 2017. Physics of metabolic organization. Phys Life Rev 20, 1–39. https://doi.org/10.1016/j.plrev.2016.09.001.
Kooijman, S.A.L.M., 2010. Dynamic energy budget theory for metabolic organisation, 3rd ed. Cambridge university press.
Koubbi, P., Ozouf-Costaz, C., Goarant, A., Moteki, M., Hulley, P.A., Causse, R., Dettai, A., Duhamel, G., Pruvost, P., Tavernier, E., et al., 2010. Estimating the biodiversity of the East Antarctic shelf and oceanic zone for ecoregionalisation: example of the ichthyofauna of the CEAMARC (Collaborative East Antarctic Marine Census) CAML surveys. Polar Sci 4 (2), 115–133.
IPCC, 2014: Climate Change 2014: Synthesis Report. Contribution of Working Groups I, II and III to the Fifth Assessment Report of the Intergovernmental Panel on Climate Change [Core Writing Team, R.K. Pachauri and L.A. Meyer (eds.)]. IPCC, Geneva, Switzerland, 151 pp. https://www.ipcc.ch/report/ar5/syr/ Accessed November 2019.
Lang, J., 1967. Contribution à l'étude sédimentologique du golfe du Morbihan: iles Kerguelen-Terres australes et antarctiques françaises. Ph. D. Dissertation, Université de Paris.
Lang, J., 1971. Contribution à l'étude sédimentologique du Golfe du Morbihan (Iles Kerguelen). Comité National Français des Recherches Antarctiques 29.
Lawrence, J.M., Lawrence, A.L., Giese, A.C., 1966. Role of the gut as a nutrient-storage organ in the purple sea urchin (*Strongylocentrotus purpuratus*). Physiol. Zool. 39 (4), 281–290.
Ledoux, J.B., Tarnowska, K., Gerard, K., Lhuillier, E., Jacquemin, B., Weydmann, A., Féral, J.P., Chenuil, A., 2012. Fine-scale spatial genetic structure in the brooding sea urchin *Abatus cordatus* suggests vulnerability of the Southern Ocean marine invertebrates facing global change. Polar Biol. 35, 611–623. https://doi.org/10.1007/s00300-011-1106-y.
Lika, K., Kearney, M.R., Freitas, V., van der Veer, H.W., van der Meer, J., Wijsman, J.W. M., Pecquerie, L., Kooijman, S.A.L.M., 2011a. The "covariation method" for estimating the parameters of the standard Dynamic Energy Budget model I: philosophy and approach. J. Sea Res. 66 (4), 270–277. https://doi.org/10.1016/j.seares.2011.07.010.
Lika, K., Kearney, M.R., Kooijman, S.A., 2011b. The "covariation method" for estimating the parameters of the standard Dynamic Energy Budget model II: properties and preliminary patterns. J. Sea Res. 66 (4), 278–288. https://doi.org/10.1016/j.seares.2011.09.004.
Magniez, P., 1979. Modalités de l'incubation chez Abatus cordatus (Verrill), oursin endémique des îles Kerguelen. In: Jangoux, M. (Ed.), Echinoderms—present and past. Balkema Press, Rotterdam, pp. 399–403.
Magniez, P., 1980. Le cycle sexuel d'Abatus cordatus (Echinoidea: spatangoida): modalités d'incubation et évolution histologique et biochimique des gonades. Ph. D. Dissertation, Université Pierre et Marie Curie, Paris.
Magniez, P., 1983. Reproductive cycle of the brooding echinoid *Abatus cordatus* (Echinodermata) in Kerguelen (Antarctic Ocean): changes in the organ indices, biochemical composition and caloric content of the gonads. Mar. Biol. 74 (1), 55–64. https://doi.org/10.1007/BF00394275.
Magniez, P., Féral, J.P., 1988. The effect of somatic and gonadal size on the rate of oxygen consumption in the subantarctic echinoid *Abatus cordatus* (Echinodermata) from Kerguelen. Comparative Biochemistry and Physiology Part A: Physiology 90 (3), 429–434. https://doi.org/10.1016/0300-9629(88)90214-9.
Malishev, M., Bull, C.M., Kearney, M.R., 2018. An individual-based model of ectotherm movement integrating metabolic and microclimatic constraints. Methods in Ecology and Evolution 9, 472–489. https://doi.org/10.1111/2041-210X.12909.
Marques, G.M., Augustine, S., Lika, K., Pecquerie, L., Domingos, T., Kooijman, S.A., 2018. The AmP project: comparing species on the basis of dynamic energy budget parameters. PLoS Comput. Biol. 14 (5), e1006100.
Martin, B.T., .Zimmer, E.I., .Grimm, V., & Jager, T., 2010. DEB-IBM User Manual: dynamic Energy Budget theory meets individual-based modelling: a generic and accessible implementation. Available at https://www.bio.vu.nl/thb/deb/deblab/debibm/DEB_IBM_manual.pdf.
Martin, B.T., Zimmer, E.I., Grimm, V., Jager, T., 2012. Dynamic Energy Budget theory meets individual-based modelling: a generic and accessible implementation. Methods in Ecology and Evolution 3, 445–449. https://doi.org/10.1111/j.2041-210X.2011.00168.x.
McClanahan, T., Kurtis, J.D., 1991. Population regulation of the rock-boring sea urchin *Echinometra mathaei* (de Blainville). J. Exp. Mar. Biol. Ecol. 147, 121–146. https://doi.org/10.1016/0022-0981(91)90041-T.
Mespoulhé, P., 1992. Morphologie d'un échinide irrégulier subantarctique de l'archipel des Kerguelen: ontogenèse, dimorphisme sexuel et variabilité. Ph. D. Dissertation, Université de Bourgogne, Dijon.
Michel, L., David, B., Dubois, P., Lepoint, G., De Ridder, C., 2016. Trophic plasticity of Antarctic echinoids under contrasted environmental conditions. Polar Biol. 39, 913–923. https://doi.org/10.1007/s00300-015-1873-y.
Murphy, E., Hofmann, E., 2012. End-to-end in Southern Ocean ecosystems. Curr Opin Environ Sustain 4, 264–271. https://doi.org/10.1016/j.cosust.2012.05.005.
Orejas, C., Gili, J., López-González, P.J., Arntz, W., 2001. Feeding strategies and diet composition of four Antarctic cnidarian species. Polar Biol. 24, 620–627. https://doi.org/10.1007/s003000100272.
Peck, L.S., Barnes, D.K.A., Willmott, J., 2005. Responses to extreme seasonality in food supply: diet plasticity in Antarctic brachiopods. Mar. Biol. 147 (2), 453–463. https://doi.org/10.1007/s00227-005-1591-z.
Poulin, E., Féral, J.P., 1994. The fiction and the facts of Antarctic brood protecting: population genetics and evolution of schizasterid echinoids. In: David, B., Guille, A., Féral, J.P., Roux, M. (Eds.), Echinoderms through Time. A.A.Balkema Publishers, Rotterdam, pp. 837–843.
Poulin, E., Féral, J.P., 1995. Pattern of spatial distribution of a brood-protecting schizasterid echinoid, *Abatus cordatus*, endemic to the Kerguelen Islands. Mar. Ecol. Prog. Ser. 118, 179–186. https://doi.org/10.3354/meps118179.
Poulin, E., 1996. Signification adaptative et conséquences évolutives de l'incubation chez un invertébré marin benthique subantarctique, Abatus cordatus (Verrill, 1876) (Echinodermata: spatangoida). Ph. D. Dissertation, Université Montpellier II, Montpellier.
Poulin, E., Féral, J.P., 1998. 1998 Genetic structure of the brooding sea urchin Abatus cordatus, an endemic of the subantarctic Kerguelen Island. Echinoderms: San Francisco. Balkema, Rotterdam. Mooi & TelfordISBN 90 5410 929 7.
Railsback, S.F., Grimm, V., 2019. Agent-based and Individual-based Modeling: A Practical Introduction. Princeton university press.
Saraiva, S., Van der Meer, J., Kooijman, S.A.L.M., Ruardij, P., 2014. Bivalves: from individual to population modelling. J. Sea Res. 94, 71–83. https://doi.org/10.1016/j.seares.2014.06.004.
Saucède, T., 2020. Proteker 8 cruise report. Summer campaign 2019-2020. 7th Nov. 2019 - 3rd Jan. 2020. 39 pp. [in French]. http://www.proteker.net/Campagne-ddd-ete-2019.html?lang=en.
Schatt, P., 1985. Développement et croissance embryonnaire de l'oursin incubant *Abatus cordatus* (Echinoidea: spatangoida). Ph. D. Dissertation, Université Pierre et Marie Curie, Paris.
Schatt, P., Féral, J.P., 1991. The brooding cycle of *Abatus cordatus* (Echinodermata: spatangoida) at Kerguelen islands. Polar Biol. 11 (5), 283–292. https://doi.org/10.1007/BF00239020.
Schatt, P., Féral, J.P., 1996. Completely direct development of *Abatus cordatus*, a brooding schizasterid (Echinodermata: echinoidea) from Kerguelen, with description of perigastrulation, a hypothetical new mode of gastrulation. Biol. Bull. 190, 24–44. https://doi.org/10.2307/1542673.
Shulman, M.J., 1990. Aggression among sea urchins on Carribean coral reefs. J. Exp. Mar. Biol. Ecol. 140 (3), 197–207. https://doi.org/10.1016/0022-0981(90)90127-X.
Snelgrove, P.V.R.&, Butman, C.A., 1994. Animal-sediment relationships revisited: cause versus effect. Oceanography and Marine Biology: an Annual Review 32, 111–177.
Sousa, T., Domingos, T., Kooijman, S.A.L.M., 2008. From empirical patterns to theory: a formal metabolic theory of life. Philosophical Transactions of the Royal Society B: Biological Sciences 363 (1502), 2453–2464. https://doi.org/10.1098/rstb.2007.2230.
Stenni, B., Curran, M.A., Abram, N., Orsi, A., Goursaud, S., Masson-Delmotte, V., Neukom, R., Goosse, H., Divine, D., van Ommen, T., et al., 2017. . Antarctic climate variability on regional and continental scales over the last 2000 years. Climate of the Past 13, 1609–1634.
Stevenson, A., Mitchell, F., Davies, J.S., 2015. Predation has no competition: factors influencing space and resource use by echinoids in deep-sea coral habitats, as evidenced by continuous video transects. Marine Ecology 36 (4), 1454–1467. https://doi.org/10.1111/maec.12245.
Thomas, Y., Bacher, C., 2018. Assessing the sensitivity of bivalve populations to global warming using an individual-based modelling approach. Glob Chang Biol 24 (10), 4581–4597. https://doi.org/10.1111/gcb.14402.
Turner, J., Barrand, N.E., Bracegirdle, T.J., Convey, P., Hodgson, D.A., Jarvis, M., Jenkins, A., Marshall, G., Meredith, M.P., Roscoe, H., et al., 2014. Antarctic climate change and the environment: an update. In: Polar Record, 50. Cambridge University Press, pp. 237–259. https://doi.org/10.1017/S0032247413000296.
Uthicke, S., Liddy, M., Nguyen, H.D., Byrne, M., 2014. Coral Reefs 33 (3), 831–845. https://doi.org/10.1007/s00338-014-1165-y.
van der Meer, J., 2006. An introduction to Dynamic Energy Budget (DEB) models with special emphasis on parameter estimation. J. Sea Res. 56 (2), 85–102. https://doi.org/10.1016/j.seares.2006.03.001.
Vlaeminck, K., Viaene, K.P.J., Van Sprang, P., Baken, S., De Schamphelaere, K.A.C., 2019. The use of mechanistic population models in metal risk assessment: combined Effects of Copper and Food Source on *Lymnaea stagnalis* Populations. Environmental Toxicology and Chemistry 38, 1104–1119. https://doi.org/10.1002/etc.4391.
Waller, C.L., Overall, A., Fitzcharles, E.M., Griffiths, H., 2017. First report of *Laternula elliptica* in the Antarctic intertidal zone. Polar Biol. 40, 227–230. https://doi.org/10.1007/s00300-016-1941-y.
Wilensky, U., 1999. NetLogo. Center for Connected Learning and Computer-Based Modeling. Northwestern University, Evanston, IL. http://ccl.northwestern.edu/netlogo/. accessed February 2019.
Xavier, J.C., Brandt, A., Ropert-Coudert, Y., Badhe, R., Gutt, J., Havermans, C., Jones, C., Costa, E.S., Lochte, K., Schloss, I.R., Kennicutt I.I, M.C., Sutherland, W.J., 2016. Future challenges in southern ocean ecology research. Front Mar Sci 3, 94. https://doi.org/10.3389/fmars.2016.00094.